AD
A086511

END
DATE
FILMED
8-80
DTIC

ATC Report No. R-92000/0CR-31

Contract No. N00019-78-C-0491

LEVEL II

FATIGUE AND FRACTURE OF ULTRAHIGH STRENGTH STEEL AND TITANIUM ROLL-BONDED AND DIFFUSION-BONDED LAMINATES

L. E. Sloter

D. H. Petersen

Vought Corporation Advanced Technology Center
Dallas, Texas 75266

DTIC
SELECTED
JUL 1 5 1980

A

May 1980

Final Report for Period 25 September 1978 – 25 March 1980

Approved for public release; distribution unlimited

Prepared for:

Department of the Navy
Naval Air Systems Command
Washington, D.C. 20361

⊕ **VOUGHT CORPORATION**
advanced technology center

80 7 14 027

REPORT DOCUMENTATION PAGE		READ INSTRUCTIONS BEFORE COMPLETING FORM
1. REPORT NUMBER	2. GOVT ACCESSION NO. AD-A086 511	3. RECIPIENT'S CATALOG NUMBER
4. TITLE (and Subtitle) Fatigue and Fracture of Ultrahigh Strength Steel and Titanium Roll-Bonded and Diffusion-Bonded Laminates		5. TYPE OF REPORT & PERIOD COVERED Final Report. 25 September 78 – 25 March 1980
		6. PERFORMING ORG. REPORT NUMBER R-92000/0CR-31
7. AUTHOR(s) L. E. Sloter D. H. Petersen		8. CONTRACT OR GRANT NUMBER(s) N00019-78-C-0491
9. PERFORMING ORGANIZATION NAME AND ADDRESS Vought Corporation Advanced Technology Center P. O. Box 226144 Dallas, Texas 75266		10. PROGRAM ELEMENT, PROJECT, TASK AREA & WORK UNIT NUMBERS
11. CONTROLLING OFFICE NAME AND ADDRESS Department of the Navy Naval Air Systems Command Washington, D. C. 20361		12. REPORT DATE May 1980
		13. NUMBER OF PAGES 72
14. MONITORING AGENCY NAME & ADDRESS(if different from Controlling Office)		15. SECURITY CLASS. (of this report) Unclassified
		15a. DECLASSIFICATION/DOWNGRADING SCHEDULE

16. DISTRIBUTION STATEMENT (of this Report)

Approved for public release; distribution unlimited

17. DISTRIBUTION STATEMENT (of the abstract entered in Block 20, if different from Report)

18. SUPPLEMENTARY NOTES

19. KEY WORDS (Continue on reverse side if necessary and identify by block number)

Alloy 300M, Crack Arrest, Crack Divider, Damage Tolerance, Fatigue Failure, Fracture Toughness, Metal Laminates, Plane Strain Fracture, Plane Stress Fracture, Roll bonding, Ti-6Al-4V, Ti-10V-2Fe-3Al, Ti-15V-3Cr-3Al-3Sn

20. ABSTRACT (Continue on reverse side if necessary and identify by block number)

The results of the fabrication by roll bonding of metal-metal laminates and the fatigue and fracture toughness testing of these laminates are reported and discussed. Laminate panels have been prepared from layers of steel alloy 300M interleaved with thin layers of two carbon steels and an ultrahigh carbon steel and from Ti-10V-2Fe-3Al interleaved with Ti-15V-3Cr-3Al-3Sn by roll bonding and from Ti-6Al-4V interleaved with commercially pure titanium by diffusion bonding. Both the steel and titanium alloys were heat treated

DD FORM 1473 1 JAN 73   EDITION OF 1 NOV 65 IS OBSOLETE
S/N 0102-014-6601 |

such that their maximum strengths were obtained. Through proper selection of interleaf alloys (thin layers of material bonded between primary layers of the principal alloy) and heat treatment, critical fracture toughness properties were improved by over 100% over the monolithic values at ultimate strength levels of 290 ksi (1999 MPa) for the 300M steel and 190 ksi (1310 MPa) for the Ti-10V-2Fe-3Al. This improvement brought the toughness at these strength levels to values acceptable for damage tolerant service in aerospace structures or other structures requiring high fracture toughness at high strength levels. Furthermore, the fatigue strength of simulated flawed structural items machined from laminated plate was demonstrated to be superior to the equivalent monolithic material for both the steel and titanium alloys.

TABLE OF CONTENTS

TABLE OF CONTENTS (cont'd)

PREFACE

SUMMARY

Laminate materials, in which layers of similar or dissimilar materials are bonded together, offer distinct advantages over homogeneous or monolithic materials in many applications which are fracture critical, corrosion critical, or wear critical.

Such laminates may be fabricated by various methods, such as adhesive bonding, weld cladding, diffusion bonding, explosive bonding, and roll bonding. In addition, both metals and non-metals may be bonded, although not necessarily in identical ways. Metal-metal laminates fabricated exclusively from layers of metals and metal alloys which are bonded metallurgically or chemically one to another were studied in this program. Such metal-metal laminates offer the overall advantages of all laminates and are free of the disadvantages of the thermal and environmental instability of the organic adhesives used in adhesively bonded laminates.

The present report details the results obtained on the mechanical properties of metal-metal laminates fabricated by roll bonding at elevated temperatures. The roll-bonding fabrication process was chosen because of its simplicity and, more importantly, because of its demonstratable cost effectiveness when compared to diffusion bonding or cladding in the production of large laminate plates. The principal goal of the research has been the fabrication of laminates from ultrahigh strength metal alloys with fracture toughness and fatigue and fracture properties which exceeded an equivalent monolithic alloy. The two principal alloys investigated were 300M steel and the titanium alloy, Ti-10V-2Fe-3Al. Through proper selection of interleaf alloys (thin layers of material bonded between primary layers of the principal alloy) and heat treatment, critical fracture toughness properties were improved by over 100% over the monolithic values at ultimate strength levels of 290 ksi (1999 MPa) for the 300M steel and 190 ksi (1310 MPa) for the Ti-10V-2Fe-3Al. This improvement brought the toughness at these strength levels to values acceptable for damage tolerant service in aerospace structures or other structures requiring high fracture toughness at high strength levels. Furthermore, the fatigue strength of simulated flawed structural items machined from laminated plate was demonstrated to be superior to the equivalent monolithic material for both the steel and titanium alloys.

1.0 INTRODUCTION

Laminate materials, as described herein, are composed of two or more individual material layers which have been joined to form a final laminate product (Figure 1). This continuing study has been focused on laminates in which each layer retains its individual tensile and fracture properties by maintaining its individual mechanical uniqueness. This work avoided the construction of a monolithic system from individual sheets, although such a construction is possible. In the cases reported herein all the layers were metal alloys and were joined by roll bonding or diffusion bonding at elevated temperatures. The various roll bonded laminates consisted of major layers of a primary alloy and interleaves (minor layers between the major layers) of a secondary alloy. The primary alloy is the high strength component, and the interleaf prevents fusion of the primary alloy layers into a monolithic structure. The interleaf may be high or low strength depending on the alloy system and properties desired. The layers and interleaves were roll bonded such that a well bonded multilayer plate resulted. The present report compares the mechanical properties of several high strength, high toughness steel laminates with a corresponding monolithic steel reference plate and the mechanical properties of several high strength titanium laminates with monolithic titanium. In addition, the fatigue and fracture properties of simulated structural items fabricated from a titanium laminate and a steel laminate are compared with geometrically identical monolithic items.

The unique and desirable properties of adhesively bonded laminate materials have drawn considerable attention to them and their potential structural uses.[1-21] Nevertheless, concern about the environmental stability of adhesively bonded metal laminates has generally limited their use for primary structural applications. For this reason it is desirable to substitute a metal interleaf for the adhesive in order to fabricate all metal laminates through the use of novel and efficient fabrication techniques. The joining techniques used in the program have included explosive, diffusion, and roll bonding as well as adhesive bonding as a comparison.

The metal laminates for structures program has completed its third year, and the present report covers the results obtained during the third year. The overall objective of the program has been to obtain information regarding material, configurational, and processing variables on the properties of metal
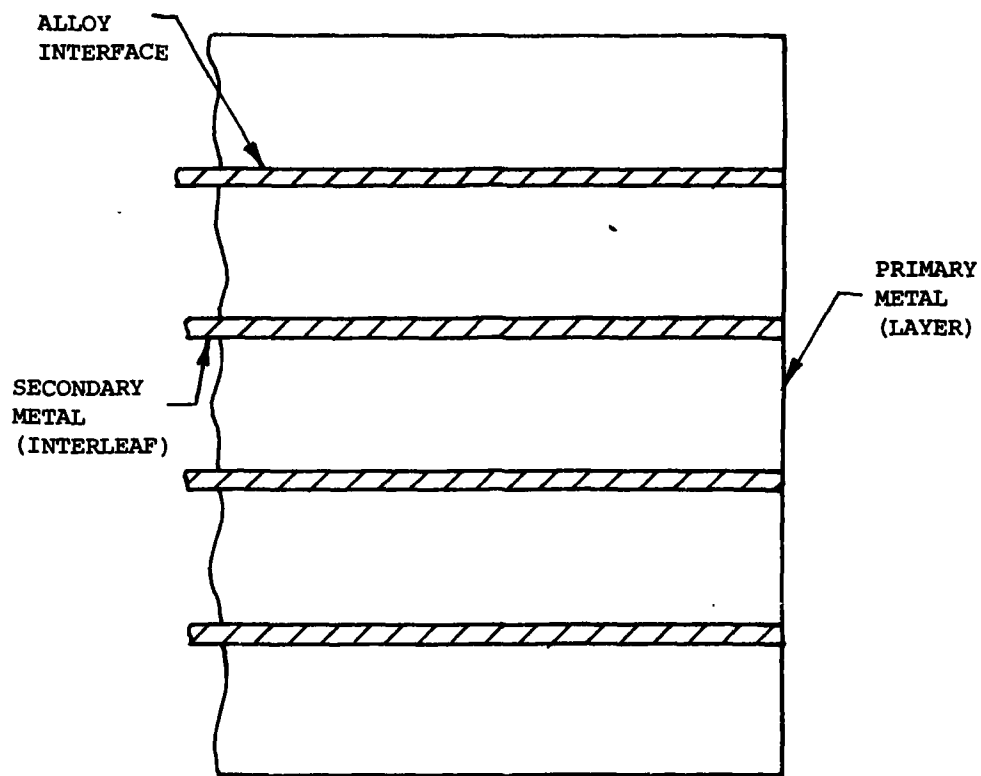
1

ALLOY
INTERFACE

PRIMARY
METAL
(LAYER)

SECONDARY
METAL
(INTERLEAF)

FIGURE 1.   SCHEMATIC METAL-METAL LAMINATE.

2

laminates, particularly with respect to fatigue and fracture. Reported herein are the results obtained for roll bonded high strength steel and titanium laminates.

The research performed during this third year of the program has been concerned with the property evaluation of roll-bonded laminates of ultrahigh strength steel and titanium alloys. Specifically, the following tasks have been performed:

    o The development of roll bonding procedures and the demonstration of the efficacy of roll bonding in the fabrication of metal laminates of high strength steel and titanium alloys.

    o The evaluation of interleaf alloy type and structure on the properties of the laminates.

    o The evaluation of heat treatment on the structure and properties of the laminates.

    o The determination of the effect of material thickness on fracture toughness, and the application of this information to laminate design.

    o The evaluation of the effects of flawed unmodified fastener holes in the alloy laminates and in the corresponding monolithic alloys.

The prior two program years were concerned with laminate fabrication and concept demonstration especially in aluminum alloy systems. During the first year of the program, seven-laminate configurations were fabricated using three processing techniques; diffusion bonding, roll bonding, and explosive bonding. The materials systems investigated were 7475 Al/1100 Al (the alloy designated to the left of the slash mark is the primary alloy; the alloy to the right, the interleaf), 7075 Al/7072 Al, and Ti-6Al-4V/6061 Al. The mechanical properties: strength, fracture toughness, and fatigue, of each laminate system were evaluated and compared with similarly heat treated monolithic alloys.[21] During the second year of the program, diffusion bonded 7475 Al/1100 Al, 7475 Al/6061 Al, 7075 Al/1100 Al, 7075 Al/7072 Al, Ti-6Al-4V/CP Ti, ultrahigh carbon steel/interstitial free iron; adhesively bonded 7475 Al and 7075 Al; and roll bonded 7475 Al/1100 Al were evaluated.[22]

2.0 EXPERIMENTAL PROCEDURE

2.1 MATERIAL SELECTION

The individual metals chosen for evaluation as laminate layers were ultrahigh strength alloys which are generally not used in structures at their highest strength levels because at these strength levels they lack sufficient fracture toughness or ductility in thick sections. Other considerations included the potential for joining these alloys by roll bonding, the existence of compatible interleaf alloys, the potential for property control through heat treatment, and commercial availability. The two alloy systems chosen for in-depth study were an ultrahigh strength (greater than 250 ksi (1724 MPa) ultimate tensile strength) medium carbon low alloy steel, 300M, and a high strength (greater than 190 ksi (1310 MPa) ultimate tensile strength) beta titanium alloy, Ti-10V-2Fe-3Al, which has recently become commercially available.[23,24]

2.1.1 Steel Alloy 300M Laminate Systems

Alloy 300M (MIL-S-8844C[25], Class 3) is an ultrahigh strength steel with excellent hardenability characteristics and moderate ductility and fracture toughness properties at tensile strengths ranging from 280 to 320 ksi (1931 - 2206 MPa). Alloy 300M is essentially a silicon modification of AISI 4340 steel (MIL-S-8844C, Class 1). The silicon addition in this alloy moderately increases the hardenability of 300M versus 4340, although it does so at the expense of graphitization resistance. Nevertheless, the added silicon improves the strength of any ferrite which forms in the alloy and most importantly, allows the quenched 300M to be tempered in the range 500° - 600°F (260° - 316°C) without the danger of 500°F embrittlement. This permits the attainment of very high strength levels in the tempered martensitic structures without the precipitous loss in toughness, especially impact strength, occasioned by the embrittlement or secondary hardening phenomenon. This beneficial result of the presence of the silicon appears to result from an alteration in the tempering kinetics of the martensite and not from any change in the transformation kinetics or hardenability. The overall specified chemical composition of 300M as well as the mill analysis of the material obtained for experiment are listed in Table 1.

4

TABLE 1.   CHEMICAL COMPOSITION OF ALLOY 300M

| ELEMENT | CONTENT, WEIGHT PERCENT | |
	SPECIFIED*[26]	MILL ANALYSIS
C	0.40 - 0.45	0.43
Mn	0.65 - 0.90	0.74
Si	1.45 - 1.80	1.64
Ni	1.65 - 2.00	1.80
Cr	0.65 - 0.90 (0.70 - 0.95)	0.90
Mo	0.30 - 0.45 (0.35 - 0.45)	0.39
V	0.05 min.	0.08
P	0.025 max. (0.010 max.)	0.006
S	0.025 max. (0.010 max.)	0.003
Cu	----	0.15
Fe	Balance	---

* MIL-S-8844C requirements which differ from commercial 300M are
   listed in parentheses.

The interleaves used in the 300M laminates were steel alloys chosen on the basis of carbon content. The three alloys selected were AISI-SAE 1020, SAE 1075, and AISI-SAE E52100. The first two of these alloys are plain carbon steels of low and high carbon content, respectively, and the third is an ultrahigh carbon bearing steel with 1% carbon. The nominal chemical compositions of these alloys are listed in Table 2. The selection of these various interleaf carbon contents permitted the evaluation of a range of interleaf strengths and ductilities while the primary metal layer (300M) properties remained the same.

2.1.2 Titanium Alloy Systems

Three titanium alloys were investigated as potential major layer materials; Ti-6Al-4V (MIL-T-9046H[27]), Ti-3Al-8V-6Cr-4Zr-4Mo, and Ti-10V-2Fe-3Al. Two alloys were used as interleaves, commercially pure titanium and Ti-15V-3Cr-3Al-3Sn. Ti-6Al-4V is a common commercial alpha-beta alloy which has been widely used for aerospace structures. Ti-3,8,6,4,4 and Ti-10,2,3, are both heat treatable high strength beta alloys as is the interleaf alloy Ti-15,3,3,3. Commercially pure titanium is greater than 99 weight percent titanium and includes principally oxygen as an impurity and strengthening element. The beta titanium alloys in general have very desirable cryogenic strength and toughness properties as well as moderate high temperature strength and excellent corrosion resistance. The specified compositions and mill analyses of the titanium alloys are listed in Table 3. The specific titanium laminate systems evaluated were Ti-6,4/CP Ti, Ti-10,2,3/Ti-15,3,3,3, and Ti-3,8,6,4,4/CP Ti. Ti-3,8,6,4,4 was also bonded to Ti-15,3,3,3 in order to evaluate dynamic recrystalization across an all beta alloy laminate interface.

2.2 LAMINATE FABRICATION

All laminates, with the exception of the Ti-6,4/CP Ti diffusion bonded laminate, were roll bonded at elevated temperatures. Commercially obtained alloy 300M plate 0.5 inch (12.7 mm) thick by 4 inches (102 mm) wide was reduced by hot rolling to approximately 0.25 inch (64 mm) thick plate. Subsequently, about half of this 0.25 inch (64 mm) plate was reduced to

6

TABLE 2. CHEMICAL COMPOSITIONS OF STEEL INTERLEAVES,
WEIGHT PERCENT. ALLOY DIGEST.[26]

	ALLOY		
ELEMENT	1020	1075	E52100
C	0.18 - 0.23	0.70 - 0.80	0.98 - 1.10
Mn	0.30 - 0.60	0.40 - 0.70	0.25 - 0.45
Si	---	---	0.15 - 0.30
Cr	---	---	0.90 - 1.15
P	0.040 max.	0.040 max.	0.025 max.
S	0.050 max.	0.050 max.	0.025 max.
Fe	Balance	Balance	Balance

TABLE 3. TITANIUM ALLOY COMPOSITIONS, WEIGHT PERCENT

ELEMENT	6Al-4V		10V-2Fe-3Al		3Al-8V-6Cr-4Zr-4Mo		15V-3Cr-3Al-3Sn		COMMERCIAL PURITY	
	Spec.[27]	Mill	Spec.[23]	Mill	Spec.[33]	Mill	Spec.[23]	Mill	Spec.[27]	Mill
Al	5.5-6.5	6.6	2.6-3.4		3.0-4.0	3.4	2.7-3.3	3.2		
V	3.5-4.5	4.3	9.0-11.0		7.5-8.5	8.2	14-16	15		
Fe	0.30	0.13	1.7-2.2		0.30 max	0.06		0.16	0.50	0.12
Cr					5.5-6.5	6.2	2.7-3.3	3.2		
Zr					3.5-4.5	4.0				
Mo					3.5-4.5	4.0				
Sn							2.7-3.3	3.1		
C	0.08 max	0.023	0.05 max		0.05 max	0.02	0.05 max	0.015	0.08 max	0.015
N	0.05 max	0.012	0.05 max		0.03 max	0.012	0.05 max	0.014	0.05 max	0.13
H	0.015 max	0.007	0.015 max			0.0014	0.015 max	0.01	0.015 max	0.004
O	0.20 max	0.14	0.13 max		0.14 max	0.084	0.15 max	0.011	0.20-0.40	0.13

8

approximately 0.125 inch (32 mm) thick plate also by hot rolling. The rolling start temperature in both cases was approximately 2100°F (1149°C). These reduced thicknesses were prepared for the determination of fracture toughness versus thickness baseline data.

Laminated plates were prepared by (1) laying up the 0.5 inch (12.7 mm) thick 300M plates with the selected interleaf sheets, (2) surface welding across the interleaves to mechanically stabilize the lay-up and seal the faying surfaces to be bonded from the atmosphere during heating and processing, and (3) roll bonding the lay-ups. This roll bonding was accomplished with a start temperature of approximately 2100°F (1149°C) and a nominal reduction of 70% - 80% overall after three to four passes through the mill. In all cases the first roll pass made on the laminate lay-up was at least of 25% reduction in thickness in order to avoid large internal tensile stresses during rolling and possible alligatoring (longitudinal splitting of the lay-up parallel to the rolling direction.) The composition of the final steel laminates and their dimensional configurations are listed in Table 4.

The process followed in fabricating the titanium alloy laminates was identical to the steel except that the laminate lay-ups were boxed in a mild steel container prior to processing and were not themselves welded. In order to prevent sticking or contamination of the lay-up by the box, a layer of titanium dioxide powder was used to separate the lay-up from the steel box. Furthermore, prior to and during the heating to the rolling temperature the boxed lay-up was purged with argon gas in order to avoid oxygen contamination of the titanium. Just prior to rolling the box was sealed by crimping the gas inlet and outlet lines. The start temperature for roll bonding all the titanium alloy laminates was 1550°F (843°C). No more than two passes were made prior to reheating. The reduction in thickness of the first pass was also at least 25%. The dimensional configurations of the titanium laminates fabricated are listed in Table 5.

TABLE 4. MAKEUP OF 300M ALLOY LAMINATES

PLATE	INTERLEAF	THICKNESS, in. (mm)		OVERALL REDUCTION IN AREA, PERCENT
		OVERALL	LAYERS/INTERLEAVES	
A	E52100	0.255 (6.48)	300M/E52100/300M 0.117/0.020/0.118 (2.97/0.51/3.00)	70
B	1020	0.499 (12.68)	300M/1020/300M/1020/300M 0.160/0.010/0.159/0.011/0.159 (4.06/0.25/4.04/0.28/4.04)	70
C	1075	0.491 (12.47)	300M/1075/300M/1075/300M 0.151/0.021/0.150/0.019/0.150 (3.84/0.53/3.81/0.48/3.81)	70
L	1020	0.533 (13.54)	300M/1020/300M/1020/300M/1020/300M 0.123/0.014/0.123/0.014/0.122/0.014/0.123 (3.12/0.36/3.12/0.36/3.10/0.36/3.12)	60

TABLE 5. MAKEUP OF TITANIUM ALLOY LAMINATES

| PLATE | LAYER | INTERLEAF | THICKNESS, in. (mm) | | OVERALL REDUCTION IN AREA, PERCENT |
			OVERALL	LAYERS/INTERLEAVES	
K	Ti-3,8,6,4,4	CPTi	0.291 (7.39)	3,8,6,4,4/CP/3,8,6,4,4 0.142/0.008/0.141 (3.61/0.20/3.58)	70
V	Ti-10,2,3	Ti-15,3,3,3	0.436 (11.07)	10,2,3/15,3,3,3/10,2,3/15,3,3,3/10,2,3 0.137/0.012/0.136/0.012/0.137 (3.48/0.31/3.51/0.31/3.48)	70
I	Ti-6,4	CPTi	0.634 (16.10)	6,4/CP/6,4/CP/6,4/CP/6,4 0.119/0.009/0.119/0.011/0.119/0.011/ 0.118/0.009/0.119 (3.02/0.23/3.02/0.28/3.02/0.28/ 3.00/0.23/3.02)	less than 10

11

2.3 LAMINATE EVALUATION

Subsequent to roll bonding, each laminate plate was evaluated for the structural integrity of the layer interleaf bonds by ultrasonic C-scan inspection. This technique indicates the presence of an unbonded internal interface or "lamination" through the reflection of a sound wave from any such interface or lack of bond. Any areas of the roll-bonded laminate in which the bond was suspect were not used for material evaluation. In all cases, roll bonding of thin laminates was successful when adequate first pass reduction was obtained. The limitations of the laboratory scale rolling mill prevented the roll bonding of thick laminates, i.e., five inches and above. In all cases the plate ends in which there had been significant lateral deformation during rolling were discarded. In addition to ultrasonic evaluation, the titanium laminates were examined metallographically for evidence of any alpha case indicative of significant oxygen contamination. In no case was a significant alpha case observed in a well bonded laminate. All the steel and titanium laminates roll bonded without any edge cracking.

2.4 HEAT TREATMENT

All alloy systems were heat treated so as to produce strength levels which were near the practical maximum. Two basic heat treatment schedules were used for the 300M systems - quenched and tempered (Q&T) and bay-quenched and tempered (bay-Q&T). Several steel specimens were also tested in the normalized condition for comparison. The details of these heat treatments are contained in Table 6. All the titanium alloy systems were tested in the solution treated and aged (STA) condition. The details of the titanium heat treatments are listed in Table 7. In the case of the titanium alloys, considerable care was exercised through protective wrapping and treating in an argon atmosphere to prevent oxygen contamination during heat treating.

2.5 MECHANICAL TESTING

Following heat treatment the mechanical properties of all alloy laminates and monolithic materials were evaluated through tensile and fracture toughness testing.

12

TABLE 6.   300M HEAT TREATMENTS.

NORMALIZED:	1600°F (871°C) for 1 hour, Air Cool.
QUENCHED AND TEMPERED:	1600°F (871°C) for 1 hour, Oil Quench. 575°F (302°C) for 2 hours, Air Cool. 575°F (302°C) for 2 hours, Air Cool.
BAY QUENCHED AND TEMPERED:	1600°F (871°C) for 1 hour, Down Quench to 1030°F (544°C) for 10 min., Oil Quench. 575°F (302°C) for 2 hours, Air Cool. 575°F (302°C) for 2 hours, Air Cool.

TABLE 7.   TITANIUM ALLOY HEAT TREATMENTS.

| ALLOY(S)	TREATMENT
Ti-10V-2Fe-3Al Ti-15V-3Cr-3Al-3Sn	STA 4: 1450°F (788°C) for 1 hour, water quench 950°F (510°) for 4 hours, air cool STA 8: 1400°F (760°C) for 1 hour, water quench 900°F (482°C) for 8 hours, air cool STA 16: 1400°F (760°C) for 1 hour, water quench 900°F (482°C) for 16 hours, air cool
Ti-3Al-8V-6Cr-4Zr-4Mo	STA 16: 1500°F (816°C) for 1/2 hour, air cool 900°F (482°C) for 16 hours, air cool
Ti-6Al-4V	STA 6: 1700°F (927°C) for 1/4 hour, water quench 1000°F (538°C) for 6 hours, air cool

2.5.1 Tensile Properties

Tensile coupons were cut from the as-rolled or annealed material in accordance with American Society for Testing and Materials (ASTM) Standard E8 for plate.[28] Specimens were singly or severally heat treated, and tensile tests were conducted in accordance with ASTM E8.

2.5.2 Fracture Properties

The fracture toughness of laminates and monolithic materials was determined from standard (ASTM-E 399[29]) compact tension specimens. These specimens were machined prior to heat treating and then precracked in accordance with ASTM-E 399. In addition to the testing of compact tension specimens, three point bend specimens of monolithic and laminate materials were tested in order to evaluate the crack arresting properties of the laminate materials and as a secondary source of fracture toughness information for the monolithic materials. Figure 2 illustrates schematically the crack divider orientation examined via compact specimen testing with the crack arrest orientation used for three point bend testing. When sufficient material existed, compact specimens were tested in which the crack orientation was parallel to the rolling direction (TL) and perpendicular to it (LT). When there was not sufficient material, only the LT orientation was tested. All three point bend specimens were cut such that the rolling direction was perpenducular to the plane of the crack and the short transverse direction was parallel to it (LS). These orientations are illustrated schematically in Figure 3. Fracture toughness parameters were calculated from measurements of the loads and the corresponding crack opening displacements (COD) experienced by the compact and bend specimens during testing. Three toughness parameters were calculated as follows:

K_Q - the conditional fracture toughness calculated using the 95% secant load (ASTM E 339) and the calculated (COD) crack length corresponding to that load.

K_A - the apparent fracture toughness calculated using the maximum load and the same crack length as K_Q.
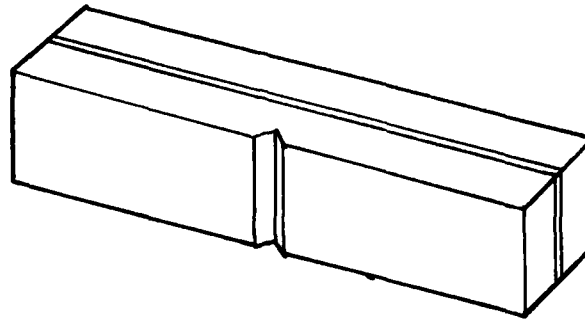
(a)
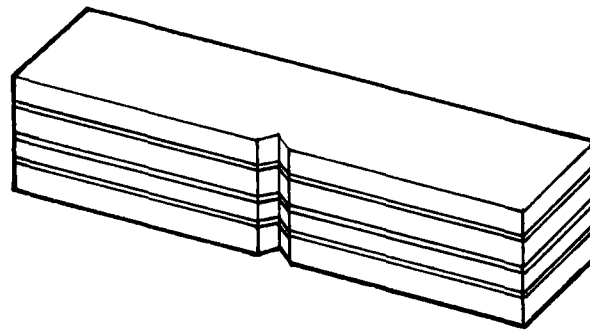
(b)

FIGURE 2. (a) CRACK ARREST AND
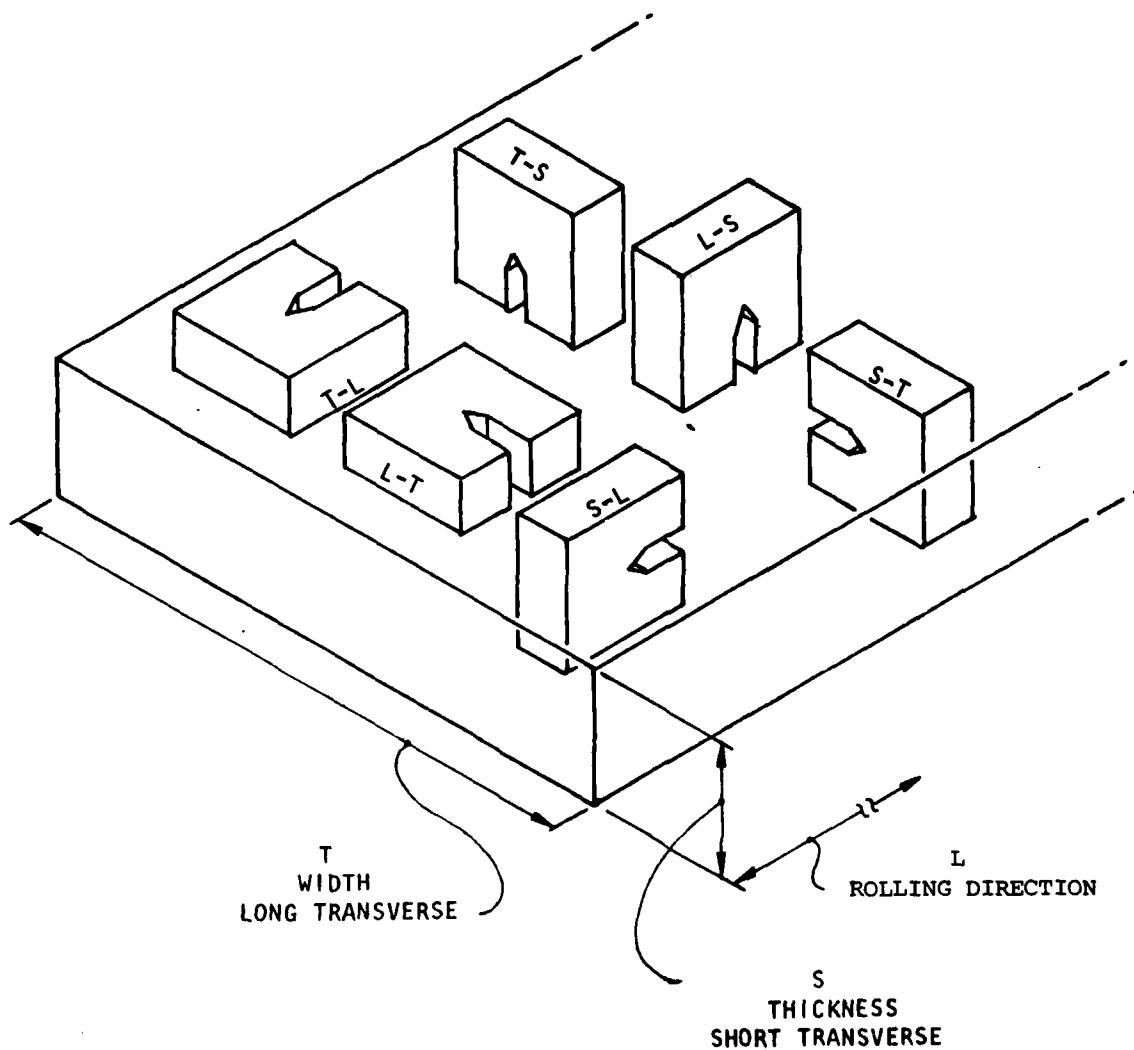   (b) CRACK DIVIDER LAMINATE ORIENTATIONS.

FIGURE 3.   SCHEMATIC ILLUSTRATION OF CRACK PLANE ORIENTATION
WITH RESPECT TO THE PLATE ORIENTATION.   AFTER
ASTM E 399[29]

K_C – the critical fracture toughness calculated using the maximum
load and the effective calculated crack length (from COD)
corresponding to maximum load.

In all cases fracture toughness K_X is defined as follows:

$$K_X = \frac{P_f}{BW^{\frac{1}{2}}} f(a/W)$$

where

P_f = load at failure or crack extension,

B   = specimen thickness,

W   = specimen width, and

a   = crack length at crack extension or failure.

In addition to the above fracture toughness parameters, the specimen strength
ratio,[29]

$$R_{SC} = \frac{2P_{max}(2W+a)}{B(W-a)^2 \sigma_y}$$

where

P_{max} = maximum load sustained by the compact specimen,

W   = specimen width,

a   = crack length,

B   = specimen thickness, and

σ_y = the 0.2% offset yield strength,

was calculated when possible.

2.6 FATIGUE AND FRACTURE EVALUATION OF A SIMULATED STRUCTURAL ITEM

In addition to the basic material property characterization involved in
the tensile and fracture toughness testing, it was considered to be desirable
to more directly compare the fatigue and fracture properties of laminates and
monolithic materials through a test specimen which simulated a practical,
structural application.

2.6.1 Item Design

An analytically simple yet structurally realistic item was required for fatigue and fracture testing. The specimen designed to meet these requirements was a tension panel with one centrally located unmodified and corner flawed fastener hole. No load was transferred through the fastener hole. The specimen design is shown schematically in Figure 4. This specimen simulates a tension skin component which contains fastener holes or a spar or other major load carrying member which also may contain fastener holes.

2.6.2 Material Selection

One steel alloy system and one titanium system were chosen for study. A 300M/1020 roll-bonded laminate was compared with a monolithic 300M panel, and a Ti-10,2,3/Ti-15,3,3,3 laminate was compared with a Ti-10,2,3 monolithic panel. In both cases the monolithic panel was machined to the same thickness as the corresponding laminate in order to facilitate comparison.

2.6.3 Testing Procedure

Each tension panel was tested by fatiguing in a servo-hydraulic testing machine to failure at a frequency of 10Hz. The maximum initial net section stress imposed on the tension panels was approximately 8% of the offset yield strength and the load ratio (P_{min}/P_{max}) was 0.1. For each panel the cycles to failure and the critical crack length at failure were recorded.
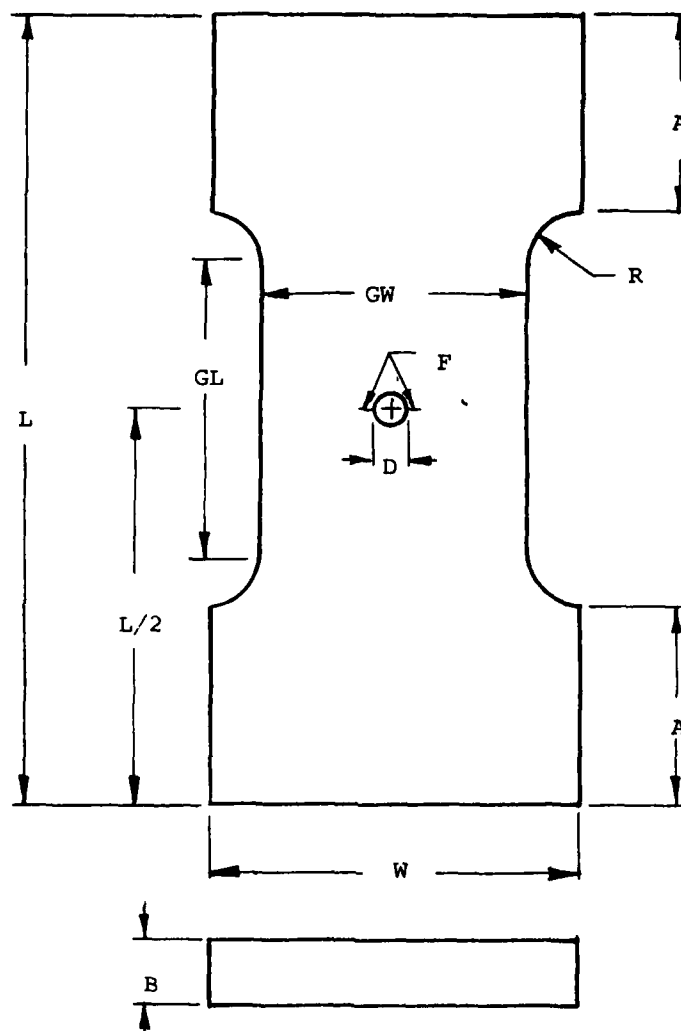
Length, L	= 6 (152.4)
Width, W	= 2.75 (69.85)
Thickness, B	= Thickness of plate
Gage Length, GL	= 1.25 (31.75)
Gage Width, GW	= 2.00 (50.8)
Grip Length, A	= 1.5 (38.1)
Radius, R	= 0.75 (19.05)
Hole Diameter	= 0.25 (6.35)
Corner Flaw, F	= 0.1 (2.54) long by 0.01 (0.254) deep

FIGURE 4.   TENSION PANEL FOR SIMULATED STRUCTURAL ITEM EVALUATION.
[DIMENSIONS ARE IN INCHES (MILLIMETERS)]

3.0 RESULTS AND DISCUSSION

3.1 STEEL ALLOYS

3.1.1 Micrography

Typical microstructures of the three 300M laminates and the various heat treatments are shown in Figures 5 - 8. In all cases the 300M alloy layer is made up of 100% tempered martensite. In Plate A the E52100 interleaf is also primarily tempered martensite but includes a large number of proeutectoid carbides. The 1020 interleaf in Plate B is primarily tempered martensite plus some acicular proeutectoid ferrite which formed during cooling. This resulted in essentially a duplex structure in which the prior austensite boundaries are outlined by continuous blocky ferrite and Widmanstatten side plates. The bay-quench and temper caused the 1020 structure to be composed of a similar acicular ferrite while tempered upper bainite replaced the pearlite. Because of the reduced transformation kinetics in the 1075 interleaves, the quench and temper resulted in 100% tempered martensite in Plate C interleaves, and the bay-quench and temper resulted in 100% tempered pearlite. The structure of the E52100, in that it is extremely fine grained, allows this alloy to deform superplastically at elevated temperatures, while the presence of the carbides prevents extensive grain growth during superplastic deformation.[30]

3.1.2 Tensile Properties

The results of the tensile testing for the various 300M systems are contained in Tables 8 and 9. Both quench and temper heat treatments resulted in yield strengths of approximately 250ksi (1724 MPa) and ultimate tensile strengths of nearly 300ksi (2068 MPa) for the monolithic 300M. The yield and ultimate strengths of the laminates were somewhat lower due to the presence of a significant volume fraction of softer interleaf in their make-up. These volume fractions were 7.8% for plate A, 4.2% for plate B, and 8.1% for plate C. It may be noted in the Table 9 that the martensitic interleaves resulted in stronger laminates than did the pearlitic or bainitic microstructures. Although the overall tensile elognations measured for the roll-bonded
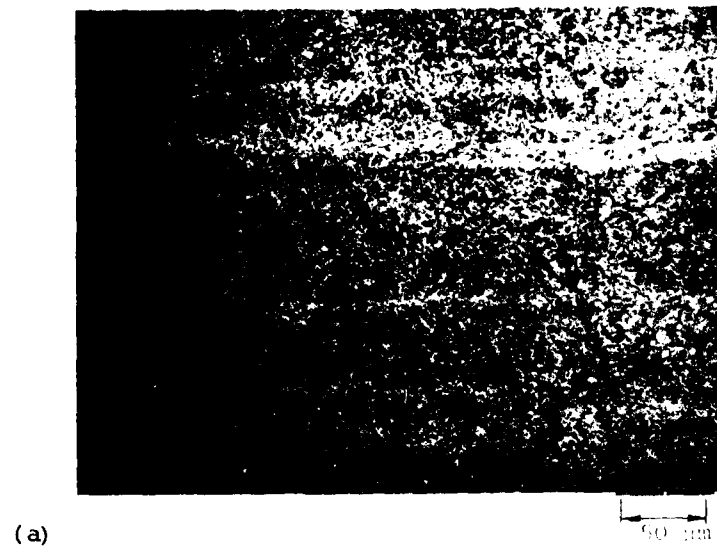
(a)

(b)

FIGURE 5. MICROSTRUCTURE OF SAMPLE IN AS-RECEIVED CONDITION.
5% NITAL ETCH. a) MAGNIFICATION 238X and b) 595X.
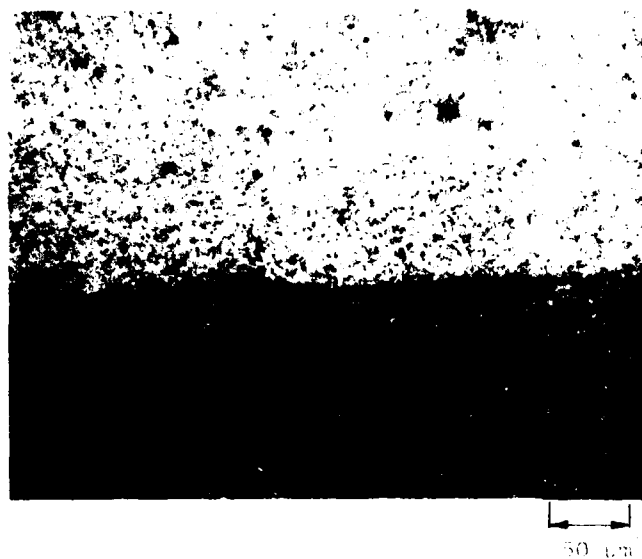
(a) PLATE A QUENCHED AND TEMPERED.
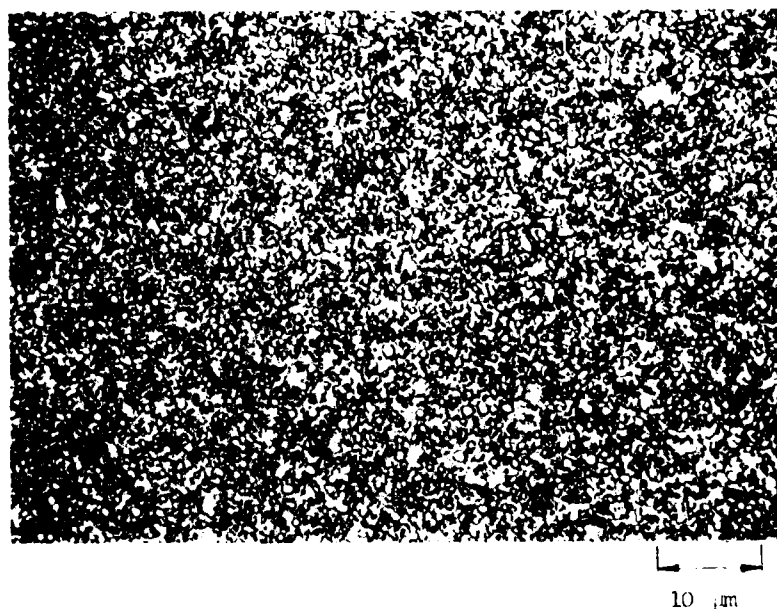
(b) E52100 QUENCHED AND TEMPERED.

FIGURE 6. (a) MICROSTRUCTURE OF PLATE A (300M/E52100)
AND (b) E52100. 300M AT TOP OF MICROGRAPH
IN (a). TRANSVERSE SECTION. 2% NITAL ETCHANT.
MAGNIFICATION: (a) 236X AND (b) 1550X
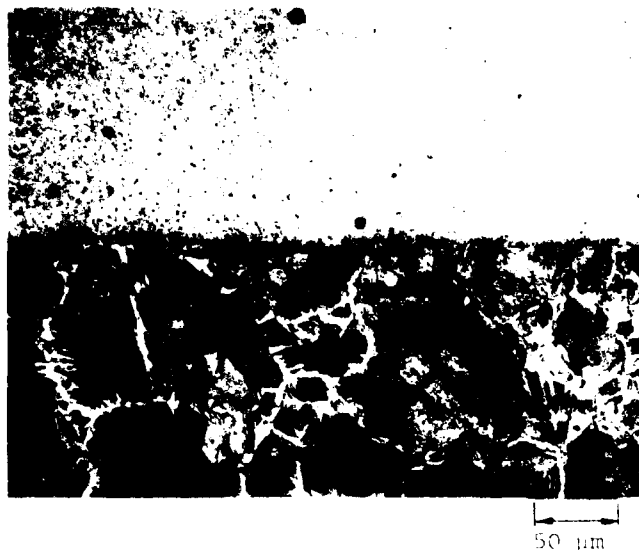
(a) QUENCHED AND TEMPERED.
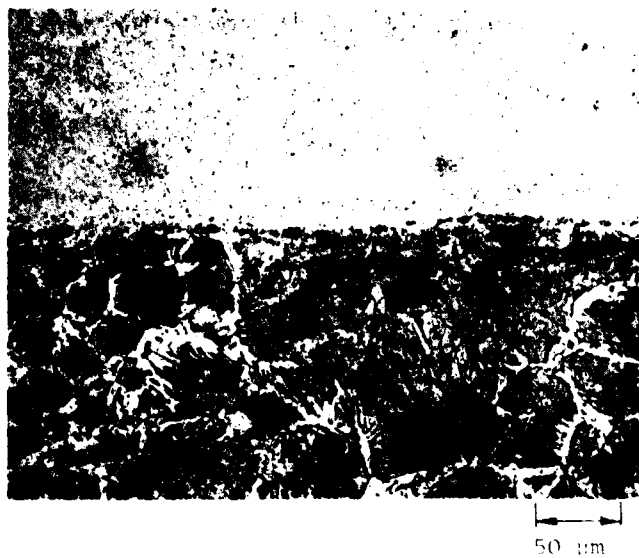
(b) RAY-QUENCHED AND TEMPERED.

FIGURE 7. MICROSTRUCTURE OF PLATE B (300M/1020). 300M
AT TOP OF MICROGRAPHS. TRANSVERSE SECTIONS.
2% NITAL ETCHANT. MAGNIFICATION: 236X

23

(a) QUENCHED AND TEMPERED.

(b) RAY-QUENCHED AND TEMPERED.

FIGURE 8. MICROSTRUCTURE OF PLATE C (300M/1075).
300M AT TOP OF MICROGRAPHS. TRANSVERSE
SECTIONS. 2% NITAL ETCHANT. MAGNIFICATION:
236X.

TABLE 8. TENSILE PROPERTIES OF MONOLITHIC 300M STEEL.

SPECIMEN, HEAT TREATMENT	0.2% OFFSET YIELD STRENGTH, ksi (MPa)	ULTIMATE TENSILE STRENGTH ksi (MPa)	TENSILE ELONGATION %	TRUE STRAIN AT FRACTURE %	UNIFORM ELONGATION %	TRUE STRAIN AT NECKING %	REDUCTION IN AREA %	TRUE STRESS AT NECKING ksi (MPa)
#1, NORM	185 (1276)	340 (2344)	9.3	19	6.6	6.4	17	362 (2496)
#2, NORM	158 (1089)	338 (2330)	12.8	41	7.3	7.0	34	362 (2496)
Average, NORM	172 (1186)	339 (2337)	11.0	30	7.0	6.7	26	362 (2496)
#1, Q & T	251 (1731)	294 (2027)	14.0	69	3.3	3.2	50	304 (2096)
#2, Q & T	248 (1710)	296 (2041)	4.5	—	3.8	3.7	—	307 (2117)
Average, Q & T	250 (1724)	295 (2034)	9.25	—	3.6	3.5	—	306 (2110)
#1, Bay - Q & T	253 (1744)	298 (2055)	14.4	70	4.4	4.3	50	311 (2144)
#2, Bay - Q & T	255 (1758)	299 (2062)	14.0	50	4.5	4.4	40	313 (2158)
Average, Bay - Q & T	254 (1751)	299 (2062)	14.0	60	4.5	4.4	45	312 (2151)

TABLE 9. TENSILE PROPERTIES OF 300M STEEL ROLL-BONDED LAMINATES

SPECIMEN, HEAT TREATMENT	0.2% OFFSET YIELD STRENGTH, ksi (MPa)	ULTIMATE TENSILE STRENGTH ksi (MPa)	TENSILE ELONGATION %	TRUE STRAIN AT FRACTURE %	UNIFORM ELONGATION %	TRUE STRAIN AT NECKING %	REDUCTION IN AREA %	TRUE STRESS AT NECKING ksi (MPa)
PLATE A, Q & T	---	260 (1793)	1.8	1.7	---	---	---	265 (1827)
PLATE A, Q & T	231 (1593)	237 (1634)	1.1	1.1	1.1	1.1	---	240 (1655)
PLATE A, Q & T AVERAGE	231 (1593)	249 (1717)	1.5	1.4	1.1	1.1	---	253 (1744)

26

TABLE 9 (CONT.). TENSILE PROPERTIES OF 300M STEEL ROLL-BONDED LAMINATES

| SPECIMEN, HEAT TREATMENT	0.2% OFFSET YIELD STRENGTH, ksi (MPa)	ULTIMATE TENSILE STRENGTH ksi (MPa)	TENSILE ELONGATION %	TRUE STRAIN AT FRACTURE %	UNIFORM ELONGATION %	TRUE STRAIN AT NECKING %	REDUCTION IN AREA %	TRUE STRESS AT NECKING ksi (MPa)
PLATE B, Q & T	232 (1600)	293 (2020)	13.2	---	4.8	4.6	---	307 (2117)
PLATE B, Q & T	213 (1469)	268 (1848)	12.6	---	4.6	4.5	---	281 (1937)
PLATE B, Q & T AVERAGE	223 (1538)	281 (1937)	12.9	---	4.7	4.6	---	294 (2027)
PLATE B, BAY - Q & T	219 (1510)	269 (1855)	11.4	---	3.8	3.7	---	279 (1924)
PLATE B, BAY - Q & T	204 (1407)	264 (1820)	13.2	---	4.4	4.3	---	275 (1896)
PLATE B, BAY - Q & T AVERAGE	212 (1462)	267 (1841)	12.3	---	4.1	4.0	---	277 (1910)
PLATE C, Q & T	233 (1606)	287 (1979)	9.6	---	4.4	4.3	---	299 (2062)
PLATE C, Q & T	241 (1662)	286 (1972)	12.1	---	4.5	4.4	---	279 (1924)
PLATE C, Q & T AVERAGE	237 (1634)	287 (1979)	10.9	---	4.5	4.4	---	289 (1993)
PLATE C, BAY - Q & T	222 (1531)	274 (1889)	11.7	---	4.4	4.3	---	286 (1972)
PLATE C, BAY - Q & T	221 (1524)	271 (1868)	13.3	---	4.8	4.6	---	283 (1951)
PLATE C, BAY - Q & T AVERAGE	222 (1531)	273 (1882)	12.5	---	4.6	4.5	---	285 (1965)
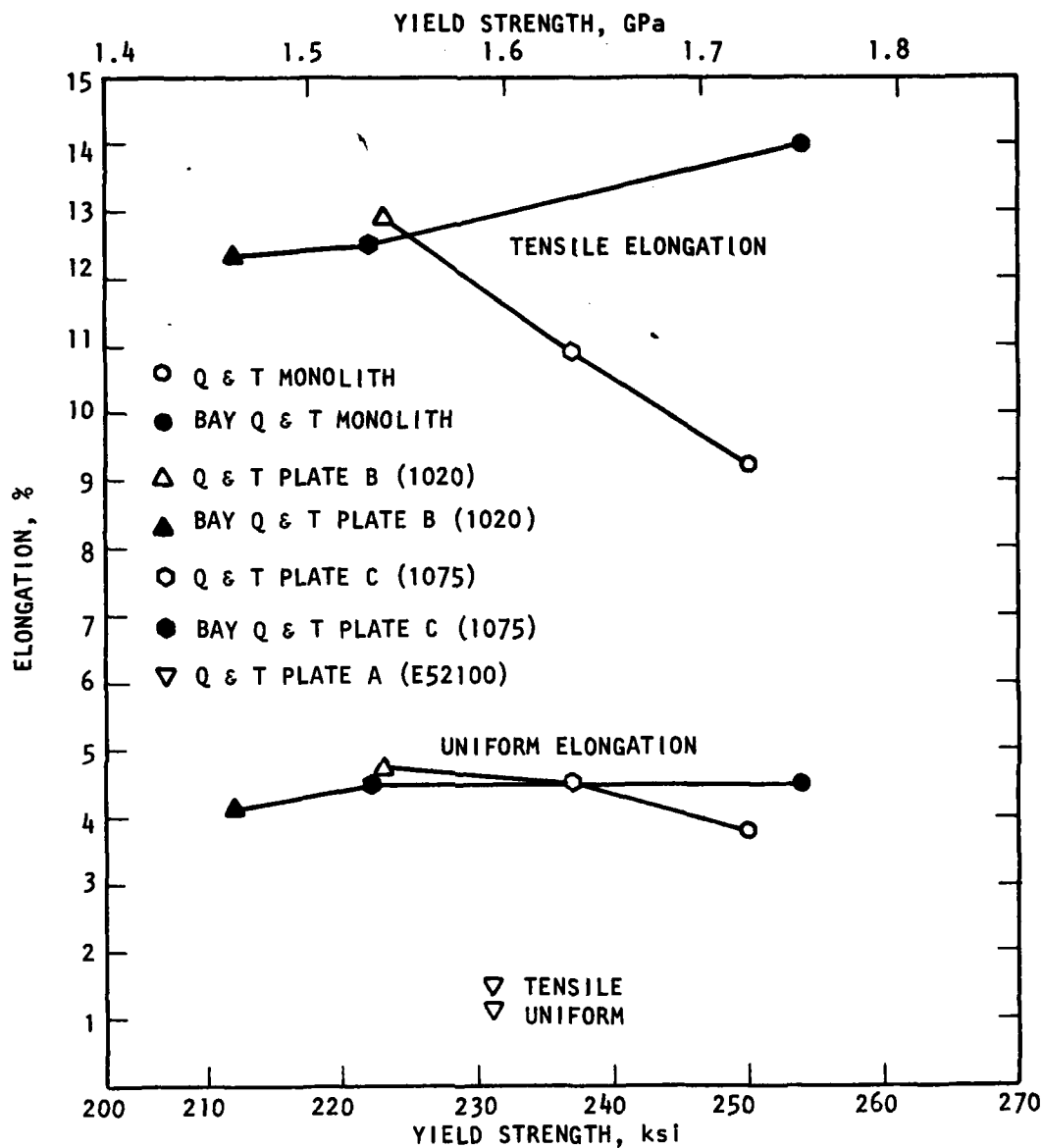
FIGURE 9. UNIFORM AND TENSILE ELONGATION VERSUS YIELD
STRENGTH FOR THE 300M ALLOY SYSTEMS.
(AVERAGE VALUES)

300M/1020 and 300M/1075 laminates were approximately equivalent to the monolithic material, their uniform elongations were consistently somewhat greater. See Figure 9. This is an important material property improvement since the uniform elongation represents the usable plastic flow of a material prior to tensile instability. This parameter can be related to the forming characteristics of metals as well as to some structural capabilities.[31]

Following the onset of tensile instability or necking the 1020 and 1075 interleaf systems delaminate in a controlled manner as shown in Figure 10. This delamination results from generation of hydrostatic tensile stresses in the necking region such that the stresses normal to the laminae pull them apart. This allows the tensile specimen to act as if it were made up of individually deforming and fracturing laminae, and allows the tensile specimen to absorb more energy during tensile deformation and fracture. Furthermore, this controlled delamination and the different plastic properties of the layer and interleaf alloys is vitally important in the Mode I fracture of the laminates and will be discussed more fully with respect to fracture toughness testing of the laminates. [It should be noted that reduction in area and true strain at fracture are not relevant to the laminates when they delaminate during tensile deformation.]

Unlike the 1020 and 1075 interleaf alloys the E52100, when used as an interleaf with 300M, decreases the tensile ductility of the resulting laminate, although the strength of the laminate is comparable to other systems (Table 9). The mechanics responsible for this behavior are clearly evident in Figure 1 . When the E52100 interleaf (center lamina in the figure) fails at approximately 1.5% overall elongation, the elastic energy released and the presence of a large central sharp flaw in the tensile specimen causes the 300M laminae on either side to fracture in essentially a flat brittle manner. The tensile behavior of the interleaf, therefore, when it has limited tensile ductility, controls the ductility of the laminate as measured by elongation or reduction in area at fracture. The controlled delamination which obtains in the soft interleaf systems and leads to enhanced uniform elongation and energy absorption does not obtain in the hard, brittle interleaf system. The tensile properties of the interleaf material must be chosen properly in order to achieve the desired tensile behavior in the laminate. The interleaf properties which have been identified to be of especial importance are the uniform elongation and the elongation at fracture or tensile elongation.

29
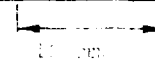
(a) LONGITUDINAL VIEW, MATING SURFACES.
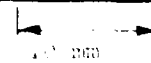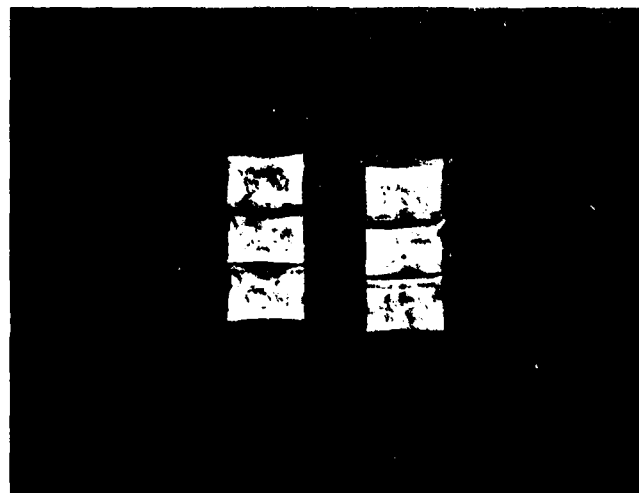
(b) TRANSVERSE VIEW, MATING SURFACES.

FIGURE 10. PLATE B (STOCK/IRON) TENSILE FRACTURE.
UPPER/LOWER AND LEFT/RIGHT. MAGNIFICATION: 2X
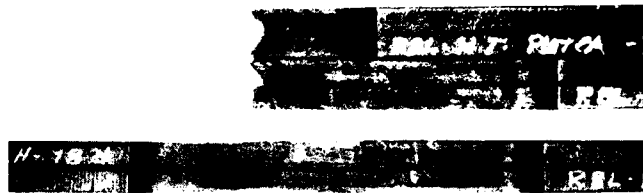
(a) LONGITUDINAL VIEW. IN THE LOWER TENSILE
THE TEST WAS TERMINATED PRIOR TO FAILURE
OF THE SECOND LAYER.

5 mm
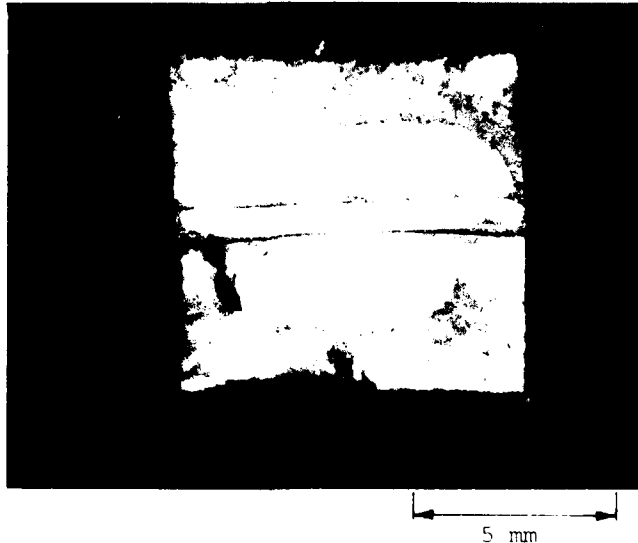
(b) TRANSVERSE VIEW

FIGURE 11. PLATE A (300M/E52100) TENSILE FRACTURES.
QUENCHED AND TEMPERED. MAGNIFICATION:
a) 1X and b) 6X.

31

3.1.3 Fracture Properties

The fracture toughness values obtained for the 300M steel systems are listed in Tables 10 and 11. In general, the conditional fracture toughness is indicative of the resistance of the material to sub-critical crack extension while the critical fracture toughness is related to the maximum ability of the material to withstand a sharp flaw and is an elastic-plastic parameter. The apparent fracture toughness is a conservative elastic-plastic parameter which relates the maximum load sustained with the initial crack length. The specimen strength ratio is a good comparator of toughness among materials when their thicknesses are approximately equal.
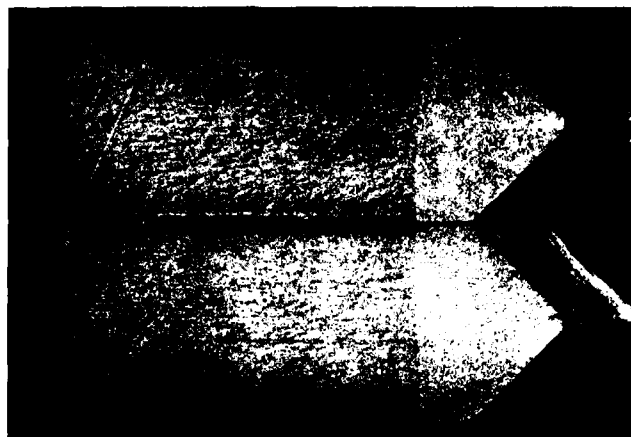
A comparison of the toughness values listed in Tables 10 and 11 reveals that the toughness is a function of both specimen thickness and heat treatment. In general, the toughness of materials decreases with increasing specimen thickness until a minimum thickness for plane strain conditions obtains. At this plane strain thickness the measured crack extension will occur under conditions of plane strain and a critical plane strain fracture toughness, K_{IC}, value will be measured. It is this limiting lower value of fracture toughness which allows the fracture behavior of large structures composed of thick sections to be accurately predicted. It also, however, is the cause of the potentially brittle fracture of thick sections. Laminates possess the ability to retain the fracture toughness inherent in thin sections in section sizes that approach or exceed those necessary for plane strain. The key toughness improvement achievable through lamination is in retaining the fracture behavior of the individual laminae. Figure 12 is a comparison of the fracture surfaces of two compact tension specimens which failed under nominally plane strain conditions. The fracture of the monolithic 300M is completely brittle as evidenced by the flat nature of the fracture surface and the absence of any appreciable shear lips. The laminate, on the other hand, has developed shear lips within each of the individual layers, and the interleaves themselves have failed ductilely by necking. The more specular triangular regions of the fracture surfaces on the right side of the fractographs are the fatigue preflaw fracture surfaces. The controlled delamination which had been demonstrated through tension testing has acted here to produce a more energy absorbing and, therefore, tougher fracture. Figure 13a graphically illustrates the general critical fracture toughness

32

TABLE 10. FRACTURE TOUGHNESS OF MONOLITHIC 300M STEEL.
COMPACT TENSION SPECIMENS.

SPECIMEN, HEAT TREATMENT	THICKNESS, in. (mm)	CONDITIONAL FRACTURE TOUGHNESS, ksi-in$^{\frac{1}{2}}$(MPa-m$^{\frac{1}{2}}$)	APPARENT FRACTURE TOUGHNESS, ksi-in$^{\frac{1}{2}}$(MPa-m$^{\frac{1}{2}}$)	CRITICAL FRACTURE TOUGHNESS, ksi-in$^{\frac{1}{2}}$(MPa-m$^{\frac{1}{2}}$)	SPECIMEN STRENGTH RATIO
#1, NORM	0.536 (13.6)	37 (41)	37 (41)	42 (46)	0.302
#1, Q & T	0.541 (13.7)	73 (80)	73 (80)	82 (90)	0.406
#4, Q & T	0.145 (3.68)	81 (89)	92 (101)	135 (148)	0.621
#5, Q & T	0.144 (3.66)	82 (90)	91 (100)	123 (135)	0.615
#6, Q & T	0.285 (7.24)	73 (80)	77 (85)	101 (111)	0.474
#1, Bay - Q & T	0.536 (13.6)	67 (74)	67 (74)	75 (82)	0.366
#2, Bay - Q & T	0.536 (13.6)	68 (75)	68 (75)	76 (84)	0.369

33

TABLE 11. FRACTURE TOUGHNESS OF 300M STEEL ROLL-BONDED LAMINATES COMPACT TENSION SPECIMENS.

SPECIMEN, HEAT TREATMENT, ORIENTATION	THICKNESS, in. (mm)	CONDITIONAL FRACTURE TOUGHNESS, ksi-in$^{\frac{1}{2}}$(MPa-m$^{\frac{1}{2}}$)	APPARENT FRACTURE TOUGHNESS, ksi-in$^{\frac{1}{2}}$(MPa-m$^{\frac{1}{2}}$)	CRITICAL FRACTURE TOUGHNESS, ksi-in$^{\frac{1}{2}}$(MPa-m$^{\frac{1}{2}}$)	SPECIMEN STRENGTH RATIO
PLATE A, Q & T, LT	0.253 (6.43)	80 (88)	88 (97)	133 (146)	0.606
PLATE A, Q & T, TL	0.254 (6.45)	78 (86)	87 (96)	129 (142)	0.603
PLATE B, Q & T, LT	0.502 (12.75)	87 (96)	97 (107)	140 (154)	0.712
PLATE B, Q & T, TL	0.500 (12.70)	88 (97)	96 (105)	133 (146)	0.670
PLATE B, BAY Q & T, TL	0.499 (12.68)	77 (85)	85 (93)	119 (131)	0.667
PLATE C, Q & T, LT	0.496 (12.60)	78 (86)	84 (92)	120 (132)	0.581
PLATE C, Q & T, TL	0491 (12.47)	82 (90)	86 (95)	120 (132)	0.515
PLATE C, BAY Q & T, LT	0.494 (12.55)	75 (82)	79 (87)	104 (114)	0.538

34

10 mm

(a) 300M QUENCHED AND TEMPERED COMPACT
TENSION SPECIMEN FRACTURE SURFACES.

10 mm

(b) PLATE B (300M/1020) QUENCHED AND TEMPERED
COMPACT TENSION FRACTURE SURFACES.

FIGURE 12. COMPARISON OF MONOLITHIC AND ROLL-BONDED LAMINATE THICK
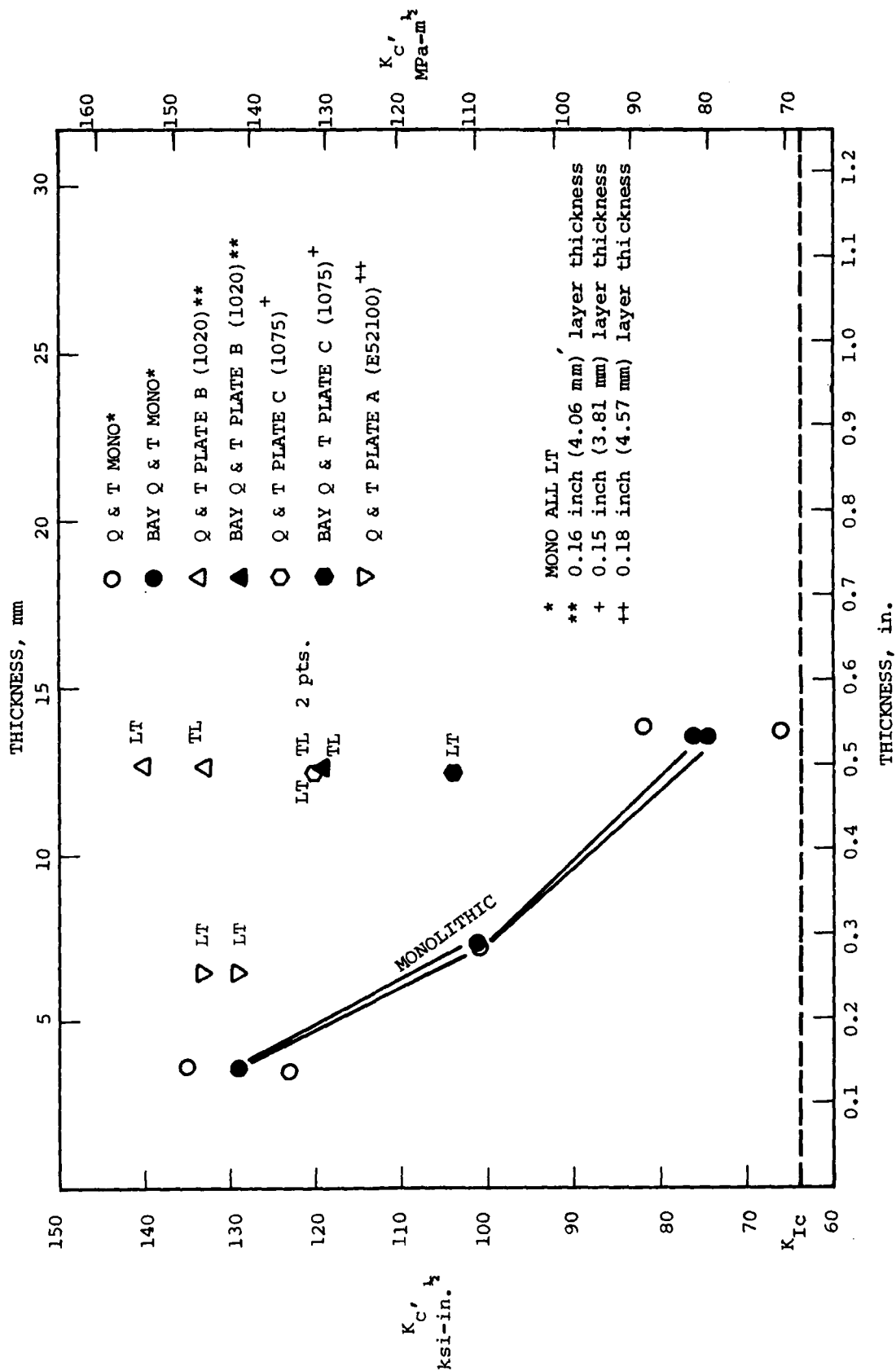SECTION FRACTURE SURFACES. MAGNIFICATION: 2X

FIGURE 13a: CRITICAL FRACTURE TOUGHNESS VERSUS THICKNESS FOR THE 300M SYSTEM.

versus thickness relationship experimentally measured for monolithic 300M steel as well as the toughness of the roll-bonded laminates, and Figure 13b, the critical fracture toughness versus tensile strength. It may be noted again that the laminates achieve toughnesses indicative of individual laminae of the equivalent thicknesses. It is further worthy of note that, although Plate A containing the E52100 interleaf had very poor tensile ductility, its fracture toughness in the crack divider orientation was also of the individual layer type and of high relative toughness. This 300M/E52100 fracture behavior is illustrated in Figure 14 in which the very brittle behavior of the E52100 interleaf may be noted.

In all cases the bay-quench and temper heat treatment resulted in slightly lower toughness when compared with a corresponding specimen in the quenched and tempered condition. This is a result of lowered toughness in the 300M itself, and is apparently occasioned by the lower final quenching temperature. [32] Although the bay-quenched and tempered laminates did achieve individual layer toughnesses, they were not as high as the quenched and tempered material and were, therefore, not pursued further experimentally.

In addition to the crack divider orientation used for the compact tension specimens, a crack arrest orientation was examined through three point bend specimens. A monolithic and a laminate three point bend specimen are shown in Figure 15a. In the case of the laminate a small fatigue precrack originating at the notch has propagated catastropically at 1870 pounds (8.32 KN) load to produce a flat, brittle failure. In the laminate a similar precrack was only able to propagate to the first interleaf where the controlled delamination of the layer and interleaf blunted the sharp crack and arrested its growth. The total load sustained by the laminate was 4800 pounds (17.8 KN), and even this load did not cause complete failure of the specimen. Load versus displacement curves for these specimens are compared in Figure 15b.

3.1.4 Structural Item Evaluation

The results of the fatigue and fracture testing of simulated structural items of 300M and 300M roll-bonded laminates are contained in Table 12. The roll-bonded laminate tested consisted of four layers of 300M interleaved with 1020. Both the laminate and monolithic specimens were quenched and tempered to approximately 250 ksi (1724 MPa) yield strength prior to fatigue testing. The laminate and monolithic panels which were cycled at 30 kip (133 kN)
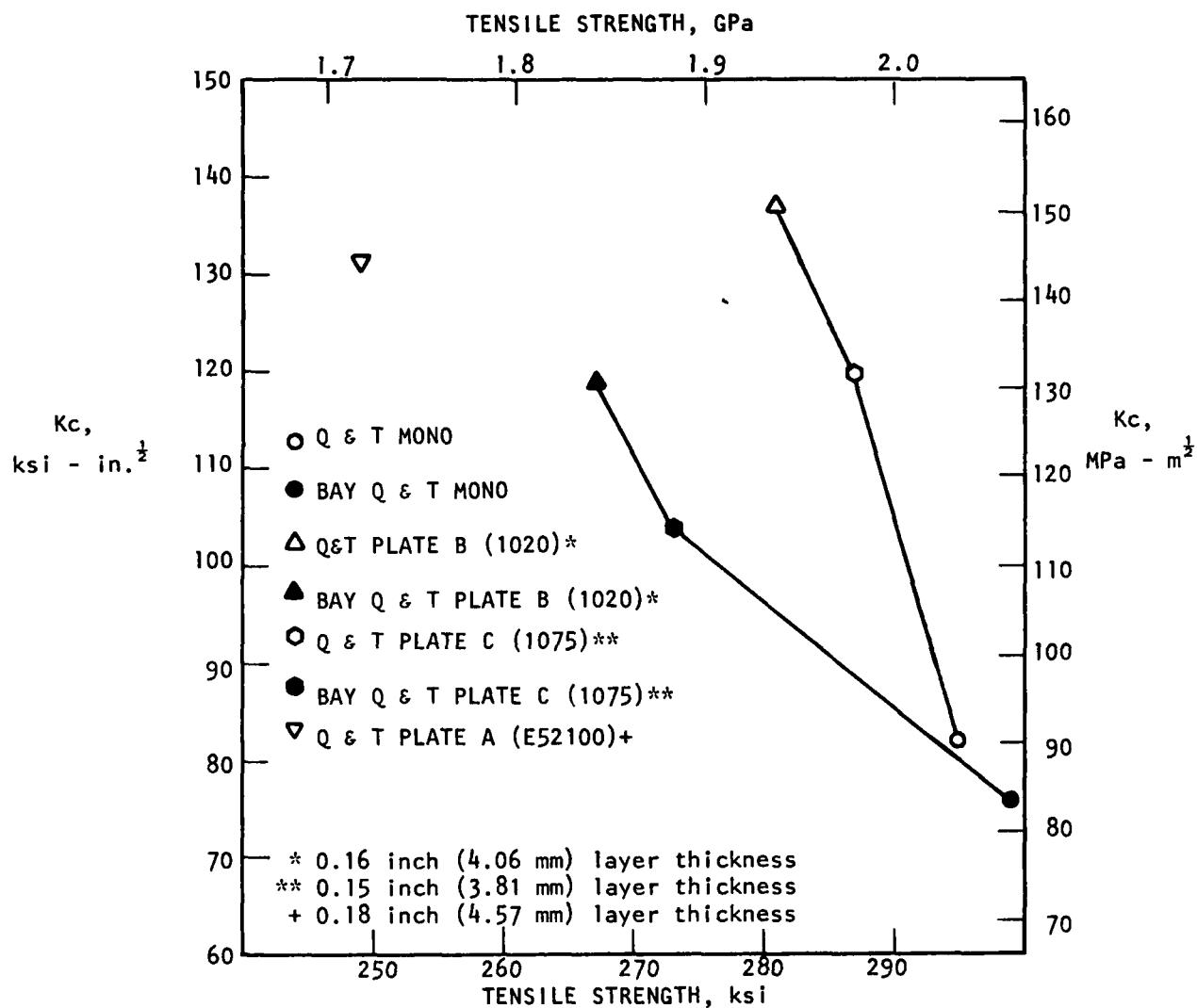
FIGURE 13b. CRITICAL FRACTURE TOUGHNESS VERSUS TENSILE
STRENGTH FOR THE 300M ALLOY SYSTEMS.
(AVERAGE VALUES)

38
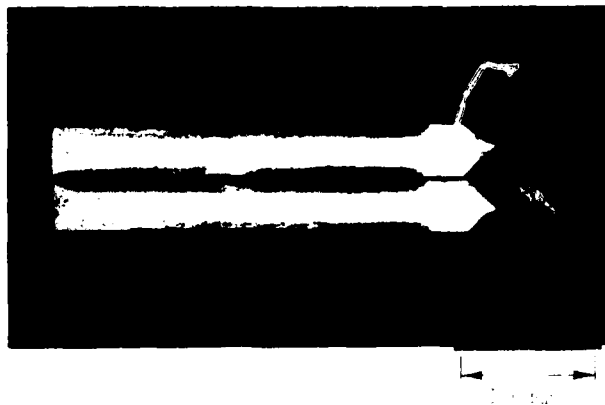
(a) 300M QUENCHED AND TEMPERED COMPACT TENSION FRACTURE SURFACES.
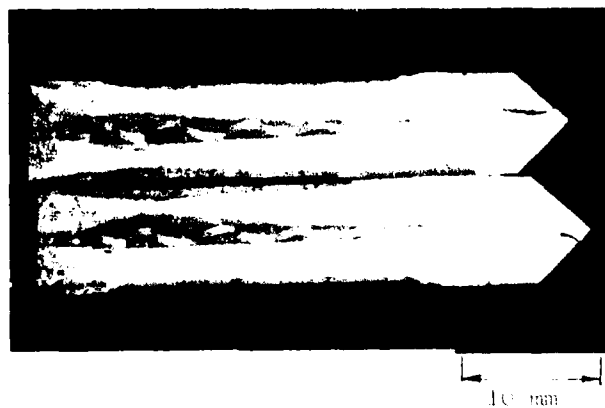
(b) PLATE A (300M/F52100) QUENCHED AND TEMPERED
COMPACT TENSION FRACTURE SURFACES.

FIGURE 14. COMPARISON OF 300M MONOLITHIC AND
PLATE A (300M/F52100) FRACTURE SURFACES.

10 mm

FIGURE 15a. 300M MONOLITHIC (TOP) THREE POINT BEND SPECIMEN
COMPARED WITH THE PLATE C (300M/1075) SPECIMEN.
MAGNIFICATION: 1X
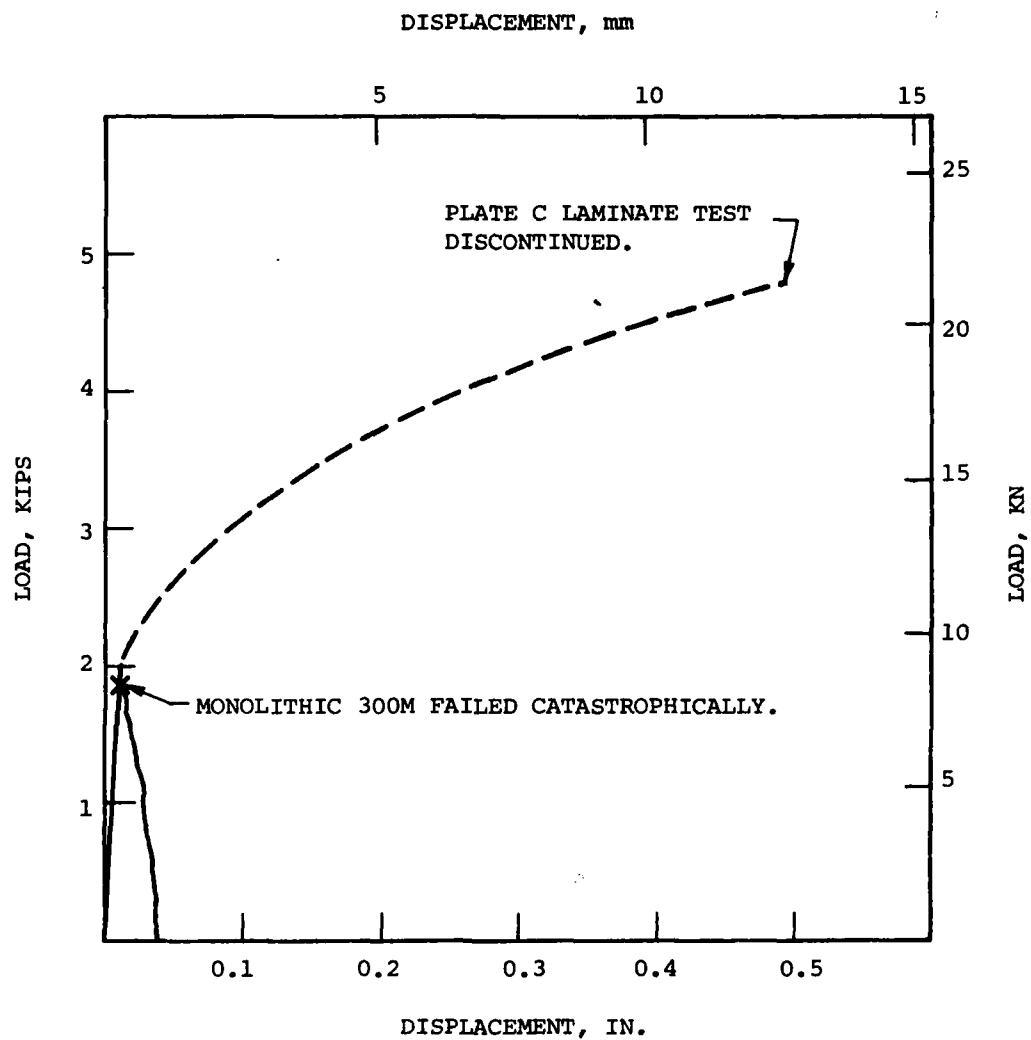
DISPLACEMENT, mm

FIGURE 15b. COMPARISON OF LOAD VERSUS RAM DISPLACEMENT
            CURVES OF 300M MONOLITHIC AND ROLL-BONDED
            LAMINATE THREE-POINT BEND SPECIMENS, CRACK
            ARREST ORIENTATION.

41

TABLE 12. 300M TENSION PANEL RESULTS.

SPECIMEN, ORIENTATION, HEAT TREATMENT	WIDTH in. (mm)	THICKNESS in. (mm)	LOAD MAX. kip (KN)	LOAD MIN. kip (KN)	CYCLES TO FAILURE
300M, MONO., LONG., Q & T	2 (50.8)	0.527 (13.39)	30 (133)	3 (13.3)	118,000
PLATE L (300M/1020), LONG., Q & T	2 (50.8)	0.533 (13.54)	30 (133)	3 (13.3)	180,000
PLATE L (300m/1020), LONG., Q & T	2 (50.8)	0.528 (13.41)	36 (160)	3.6 (16.0)	79,000

maximum load are directly comparable. As may be noted in Table 12, the laminate evidenced a 53% improvement in fatigue life over the monolithic material. Most of thi .mprovement appears to be a result of the increased over all toughness of the laminate, although there may have been some relative decrease in the fatigue crack propagation rate in the laminate especially at the highest stress intensity factor (longest crack length) levels. The tension panel fracture surfaces are compared in Figure 16. It may be noted that the controlled delamination which occurs in the compact tension specimens during fast fracture also occurs in the tension panels.

The above simulated structural item fatigue and fracture results demonstrate the efficacy of laminated structures in postponing final fracture in fatigue loading and in improving the overall fatigue performance of the item. Nevertheless, these tension panel results are not indicative of the overall fatigue crack propagation properties of laminates in the crack divider orientation since the stress intensity factor at the longer crack lengths cannot be simply calculated from linear elastic fracture mechanics criteria. In addition, the use of the corner notch in the center fastener hole does not simulate fatigue cracking in a purely crack arrest orientation either. The tension panel results should be considered to be a combination of the crack arrest and crack divider orientation and a reasonable simulation of an actual item.

3.2 TITANIUM ALLOYS

3.2.1 Micrography

The microstructure of the Ti-10,2,3 received for roll bonding is shown in Figure 17. This alloy is of the heat treatable near beta type. Two titanium laminate plates were roll bonded using Ti-3,8,6,4,4 and Ti-10,2,3 layers. The interleaves were commercial purity titanium and Ti-15,3,3,3, respectively. Micrographs of these laminates are shown in Figures 18 and 19. In all cases the canned roll bonding procedure produced a bond line which is free of contamination and which appears to have mechanical and chemical integrity. In fact, in some instances recrystallization occurred across the bond line producing an obviously true metallic bond. (Figure 20)

43
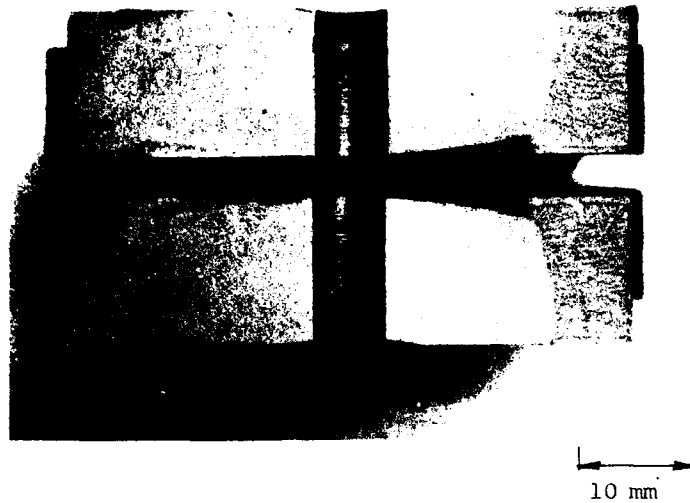
(a) 300M MONOLITHIC TENSION PANEL FRACTURE.
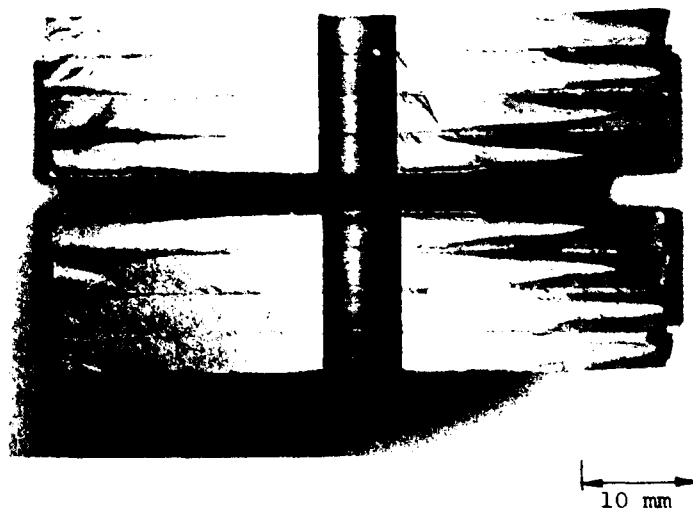
(b) PLATE L (300M/1020) TENSION PANEL FRACTURE.

FIGURE 16.   COMPARISON OF MONOLITHIC AND LAMINATE
             TENSION PANEL FRACTURE SURFACES.
             MAGNIFICATION: 1.7X.

44
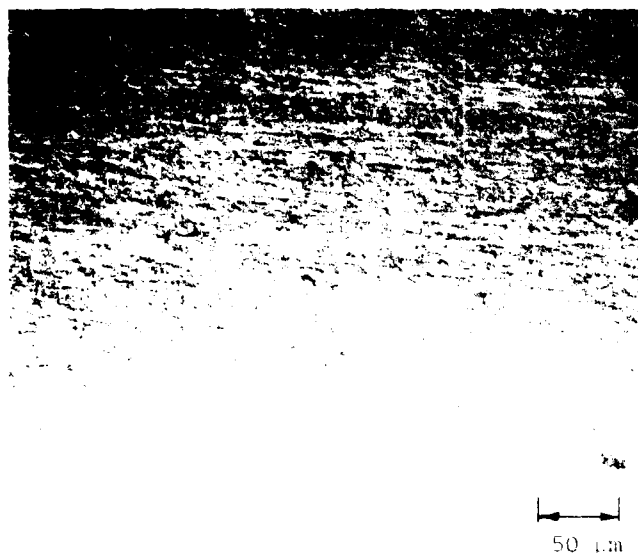
(a) ROLLING DIRECTION.
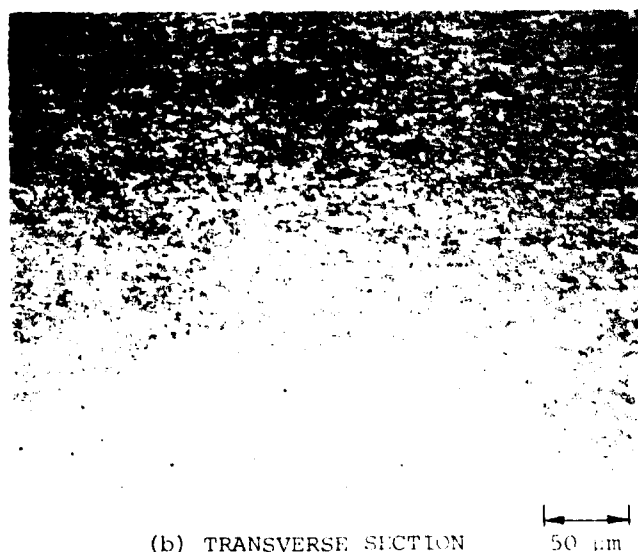
(b) TRANSVERSE SECTION   50 μm

FIGURE 17.   MICROSTRUCTURE OF Ti-10V-2Fe-3Al AS RECEIVED.
             MAGNIFICATION: 236X   HF-HNO$_3$ ETCHANT.

45

FIGURE 18. MICROSTRUCTURE OF PLATE K
(Ti-3,8,6,4,4/CP Ti). CP Ti IS CENTER LAMINA.
HF-HNO$_3$ ETCHANT. MAGNIFICATION: 236X
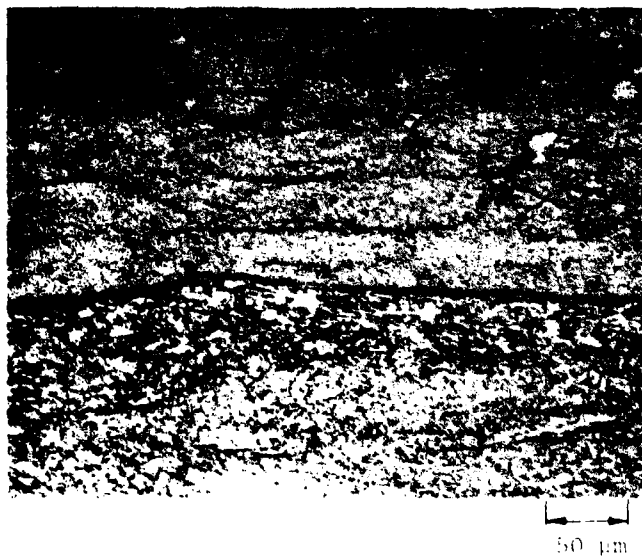
FIGURE 19. MICROSTRUCTURE OF PLATE V (Ti-10,2,3/Ti-15,3,3,3).
Ti-10,2,3 IS AT THE TOP OF THE MICROGRAPH.
TRANSVERSE SECTION. MAGNIFICATION: 236X.
HF-HNO$_3$ ETCHANT.

FIGURE 20. Ti-15,3,3,3 (TOP OF MICROGRAPH) ROLL
BONDED TO Ti-3,8,6,4,4. MAGNIFICATION:
595X. HF-HNO$_3$ ETCHANT

47

3.2.2 Tensile Properties

The tensile properties for the several titanium alloys and heat treatments examined are listed in Table 13 and the titanium laminates in Table 14. The results are basically analogous to those obtained for the steel alloys with respect to the achievement of controlled delamination during tensile deformation, and the discussion of these properties contained in the section on steels applies here also. The Ti-10,2,3/Ti-15,3,3,3 system, however presented the unique opportunity for creating a strong, brittle layer and a weaker, ductile interleaf through heat treatment. The STA 4 heat treatment which achieved this was the one most vigorously investigated, although it is not considered to be the optimum heat treatment possible for either the Ti-10,2,3 or the Ti-10,2,3/Ti-15,3,3,3 laminate. This is due to the poor overall ductility which the Ti-10,2,3 evidences in the STA 4 condition. It is once again worthy of special note that the uniform elongation of the Ti-10,2,3/Ti-15,3,3,3 laminate (Plate V) is larger than the monolithic Ti-10,2,3 in the same heat treatment condition, as is also the tensile elongation. A Plate V tensile failure is shown in Figure 21, and it may be noted there that this titanium laminate in the STA 4 heat treatment has very little tensile ductility unlike the 300M/1020 steel laminates (Figures 9 and 10).

3.2.3 Fracture Properties

The fracture toughness results obtained for the titanium alloys and titanium laminates are contained in Tables 15 and 16, respectively. In general, the toughnesses obtained for the monolithic alloys are relatively low as a result of the very high strength levels to which these alloys have been heat treated. In agreement with the results obtained for the steel alloys, the toughness decreases with increasing specimen thickness as well as with increasing strength level. The fracture toughness of the roll bonded laminates, however, is in all cases greater than the corresponding monolithic material, and, in fact, in the case of Plate V is commensurate with the toughness of the monolithic Ti-10,2,3 with a 20 ksi lower ultimate tensile strength.[24] Furthermore, even at these very high strength levels the fracture behavior of the laminate is elastic-plastic and the critical fracture toughness is considerably greater than the conditional fracture toughness.

48

TABLE 13.   TENSILE PROPERTIES OF MONOLITHIC TITANIUM ALLOYS.

TITANIUM ALLOY, HEAT TREATMENT	0.2% OFFSET YIELD STRENGTH, ksi (MPa)	ULTIMATE TENSILE STRENGTH ksi (MPa)	TENSILE ELONGATION %	TRUE STRAIN AT FRACTURE %	UNIFORM ELONGATION %	TRUE STRAIN AT NECKING %	REDUCTION IN AREA %	TRUE STRESS AT NECKING ksi (MPa)
10,2,3,STA 4	199 (1372)	199 (1372)	1.4	1.4	1.4	1.4	2.4	202 (1393)
10,2,3,STA 4	191 (1317)	193 (1331)	1.5	1.5	1.5	1.5	1.6	196 (1351)
10,2,3,STA 4 AVERAGE	195 (1344)	196 (1351)	1.5	1.5	1.5	1.5	2.0	199 (1372)
10,2,3,STA 8	184 (1269)	196 (1351)	8.3	23	3.7	3.7	20	203 (1400)
10,2,3,STA 16	180 (1241)	190 (1310)	7.2	9.8	3.7	3.6	9.3	197 (1358)
15,3,3,3,STA 4	142 (979)	152 (1048)	9.9	9.4	9.9	9.4	---	167 (1151)
15,3,3,3,STA 4	146 (1007)	159 (1096)	8.8	8.4	7.4	7.1	---	171 (1179)
15,3,3,3,STA 4 AVERAGE	144 (993)	156 (1076)	9.4	8.9	8.7	8.3	---	169 (1165)
15,3,3,3,STA 8	174 (1200)	187 (1289)	4.9	4.7	4.9	4.7	---	196 (1351)
15,3,3,3,STA 8	174 (1200)	188 (1296)	4.6	4.5	4.6	4.5	---	196 (1351)
15,3,3,3,STA 8 AVERAGE	174 (1200)	188 (1296)	4.8	4.6	4.8	4.6	---	196 (1351)
15,3,3,3,STA 16	177 (1220)	191 (1317)	3.8	---	---	---	---	---
15,3,3,3,STA 16	180 (1241)	191 (1371)	3.4	3.4	3.4	---	---	197 (1358)
15,3,3,3,STA 16 AVERAGE	179 (1234)	191 (1317)	3.6	3.4	3.4	---	---	197 (1358)
Ti-3,8,6,4,4, STA 16	206 (1420)	214 (1475)	3.0	3.0	3.0	3.0	---	220 (1517)

49

TABLE 14. TENSILE PROPERTIES OF TITANIUM ROLL-BONDED LAMINATES.

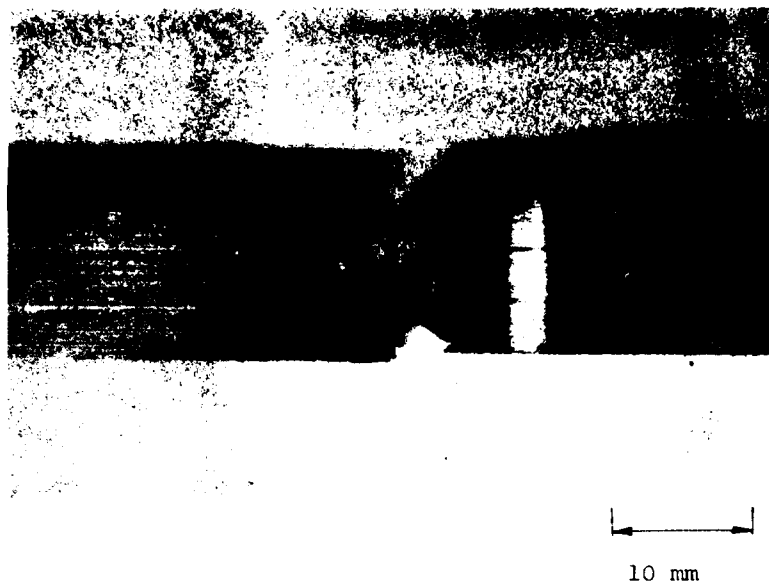| SPECIMEN, HEAT TREATMENT	0.2% OFFSET YIELD STRENGTH, ksi (MPa)	ULTIMATE TENSILE STRENGTH ksi (MPa)	TENSILE ELONG- ATION %	TRUE STRAIN AT FRACTURE %	UNIFORM ELONG- ATION %	TRUE STRAIN AT NECKING %	REDUC- TION IN AREA %	TRUE STRESS AT NECKING ksi (MPa)
PLATE V, STA 4	178 (1227)	187 (1289)	3.9	3.9	3.9	3.9	---	194 (1338)
PLATE V, STA 8	161 (1110)	185 (1276)	4.9	4.8	4.0	3.9	---	192 (1324)

10 mm

FIGURE 21.   PLATE V (Ti-10,2,3/Ti-15,3,3,3) TENSILE FAILURE.
             STA 4.   MAGNIFICATION: 2X.

51

TABLE 15. FRACTURE TOUGHNESS OF MONOLITHIC TITANIUM ALLOYS.
COMPACT TENSION SPECIMENS.

TITANIUM ALLOY, HEAT TREATMENT, ORIENTATION	THICKNESS in. (mm)	CONDITIONAL FRACTURE TOUGHNESS, ksi- in^2(MPa- m$^{\frac{1}{2}}$)	APPARENT FRACTURE TOUGHNESS, ksi- in$^{\frac{1}{2}}$(MPa- m$^{\frac{1}{2}}$)	CRITICAL FRACTURE TOUGHNESS, ksi- in$^{\frac{1}{2}}$(MPa-m$^{\frac{1}{2}}$)
10,2,3, STA 4, LT	0.132 (3.35)	34 (37.4)	34 (37.4)	37 (40.7)
10,2,3, STA 4, LT	0.133 (3.38)	36 (39.6)	36 (39.6)	38 (41.8)
10,2,3, STA 4, TL	0.447 (11.4)	37 (40.7)	38 (41.8)	42 (46.2)
10,2,3, STA 8, LT	0.133 (3.38)	42 (46.2)	44 (48.4)	54 (59.3)
10,2,3, STA 8, LT	0.134 (3.40)	42 (46.2)	46 (50.6)	71 (78.0)
10,2,3, STA 8, TL	0.448 (11.4)	26 (28.6)	28 (30.8)	36 (39.6)
3,8,6,4,4, STA 16, LT	0.485 (12.3)	27 (29.7)	27 (29.7)	27 (29.7)
3,8,6,4,4, STA 16, LT	0.486 (12.3)	25 (27.5)	26 (28.6)	34 (37.4)

52

TABLE 16. FRACTURE TOUGHNESS OF TITANIUM LAMINATES.
COMPACT TENSION SPECIMENS.

SPECIMEN, HEAT TREATMENT, ORIENTATION	THICKNESS IN. (mm)	CONDITIONAL FRACTURE TOUGHNESS, ksi- in^2(MPa- m^2)	APPARENT FRACTURE TOUGHNESS, ksi- in^2(MPa- m^2)	CRITICAL FRACTURE TOUGHNESS, ksi- in^2(MPa- m^2)
PLATE V, STA 4, LT	0.452 (11.5)	60 (65.9)	64 (70.3)	88 (96.7)
PLATE V, STA 4, TL	0.448 (11.4)	53 (58.2)	54 (59.3)	65 (71.4)
PLATE V, STA 8, TL	0.447 (11.4)	55 (60.4)	66 (72.5)	77 (84.6)
PLATE K, AS-ROLLED, LT	0.287 (7.29)	43 (47.3)	51 (56.0)	----
PLATE K, STA 16, LT	0.289 (7.34)	27 (29.7)	30 (33.0)	43 (47.3)
PLATE I, STA 6, LT	0.634 (16.1)	48 (52.8)	48 (52.8)	51 (56.0)

The toughness improvement evidenced by the roll-bonded titanium laminates is a result of controlled delamination during failure as it was in the 300M systems. This may be seen fractographically for Plate V in Figure 22. When this delamination does not obtain as in the diffusion bonded Ti-6,4/CP Ti laminate (Plate I), the laminate behaves virtually the same as a monolithic material. This explains the relatively poor toughness, approximately 50 ksi-in$^{1/2}$ (55 MPa-m$^{1/2}$), of Plate I as noted in Table 16. When the delamination occurs, however, the toughness of the individual laminae is retained in thick sections in these ultrahigh strength titanium alloys as well as in the 300M steel systems.

Perhaps the most interesting comparative results obtained in the titanium laminate systems are those obtained for Plate V in the STA 4 and STA 8 conditions. The aging kinetics of the two alloys used to make up this laminate were such that the Ti-15,3,3,3 interleaf could be overaged while the Ti-10,2,3 was being heat treated to near its maximum strength, 195 ksi (1344 MPa) yield strength. Alternatively, the interleaf could be aged to a high strength level while the Ti-10,2,3 primary layer alloy remained at a very high strength, 184 ksi (1269 MPa) yield strength. The former condition was a result of the STA 4 heat treatment while the latter, the STA 8 heat treatment. It may be observed in Table 16 that the STA 4 heat treatment resulted in approximately the same toughness for the TL orientation as the STA 8 treatment, although the yield strength of the laminate in the STA 4 condition was 17 ksi (117 MPa) greater. This result supports the conclusion drawn from the fracture toughness testing of the 300M steel laminates that the largest improvement in toughness oit as those laminates in which the ductility of the interleaves is considerally greater than the layers. In general, this will also mean that the strength of the interleaf alloy will be much less than that of the layer alloy. The crack arresting properties of the titanium laminates were also examined through the testing of three point bend specimens fabricated from Plate V. The results of these tests are shown in Figure 23 for the STA 4 and STA 8 heat treatments. The limited tensile ductility of the STA 4 condition reduced the maximum load necessary to fail the first and second layers to 1630 pounds (7.25 KN) whereas the STA 8 specimen supported 2540 pounds (11.30 KN). Nevertheless, in both cases the sharp crack propagating from the fatigue preflaw was arrested at the first interleaf, and failure of the second layer was by tensile overload. Even the failure of the second
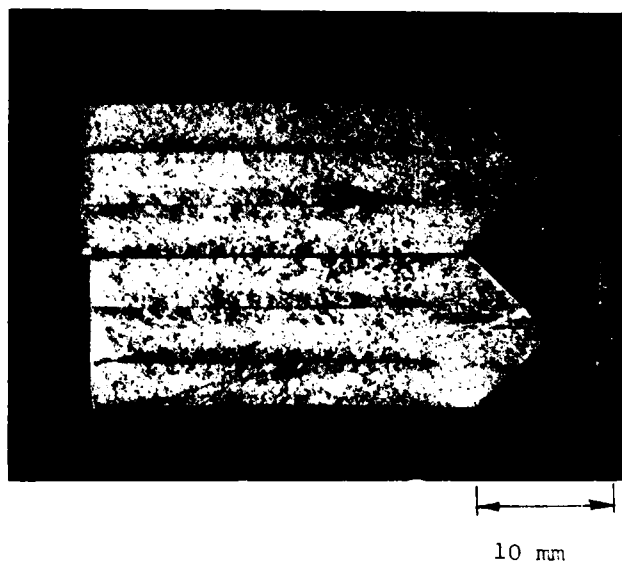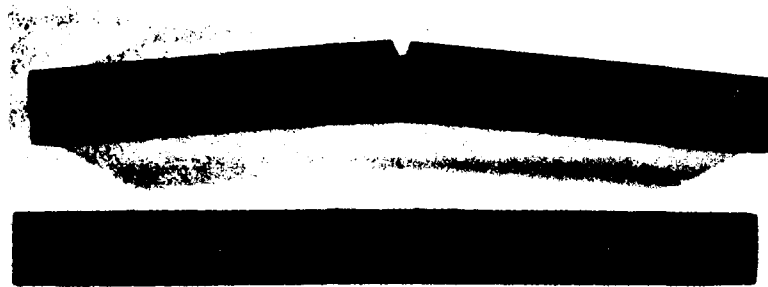
10 mm

FIGURE 22. COMPACT TENSION SPECIMEN FRACTURE OF PLATE V
(Ti-10,2,3/Ti-15,3,3,3). STA 4.
MAGNIFICATION: 2X.

55

(a) PLATE V-STA 8 AT TOP OF PHOTOGRAPH AND
PLATE V-STA 4 AT BOTTOM

(b) DETAIL OF PLATE V-STA 4 FRACTURE.

(c) DETAIL OF PLATE V-STA 8 FRACTURE

FIGURE 23. PLATE V (Ti-10,2,3/Ti-15,3,3,3) THREE POINT BEND SPECIMENS.
MAGNFICATION: a) 1X, b) 2.5X, and c) 2.5X.

56

layer and the presence of a second sharp crack therefrom did not cause complete fracture of the specimen since this propagating crack was arrested at the second interleaf. Once again, this behavior is in sharp contrast to that of Plate I (Ti-6,4/CP Ti) which failed to arrest a propagating crack in three point bending until that crack had reached the fourth interleaf. (Figure 24)

3.2.4 Structural Item Evaluation

In similar fashion to the 300M steel investigation, the overall fatigue and fracture properties of the Ti-10V-2Fe-3Al system were evaluated through the tension-tension fatigue testing of tension panels each containing one central corner notched fastener hole. The results of these tests are contained in Table 17. The failed tension panels themselves are illustrated in Figures 25 and 26. Once again the laminate panel evidenced a considerable (33%) improvement in fatigue life over the monolithic panel. This appears to be due principally to the increased toughness and concomitantly increased critical crack length of the laminate. Although the STA 4 heat treatment was chosen for the Ti-10,2,3 tension panels, this heat treatment is not considered to be the optimum for overall fatigue and fracture property improvement in the monolithic alloy or the laminate.

The results of the titanium tension panel testing are indicative of the overall efficiency of lamination in improving the fatigue and fracture properties of high strength alloys. Since the absolute value of the fracture toughness of the titanium alloys was less than the 300M steel, the tension panel results were even more representative of thick section structural item behavior. The critical crack size for the titanium panels was such that finite width effects from the limited panel size were reduced versus the steel panels. In all other respects the discussion accompanying the structural item section on steels obtains also for the titanium panels.

3.3 GENERAL DISCUSSION

Both the tensile and fracture toughness results demonstrate the improved fracture properties of ultrahigh strength steel and titanium laminates. In addition, the tension panel results demonstrate that these property improvements may be translated into improved fatigue life in a simulated

10 mm
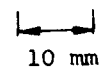
FIGURE 24. THREE POINT BEND SPECIMEN FAILURE OF PLATE I
(Ti-6,4/CP Ti) MAGNIFICATION: IX.

TABLE 17. TITANIUM TENSION PANEL RESULTS.

SPECIMEN, ORIENTATION, HEAT TREATMENT	WIDTH in.(mm)	THICKNESS in.(mm)	LOAD MAX. kip (KN)	LOAD MIN. kip (KN)	CYCLES TO FAILURE
Ti-10,2,3, MONO., TRANS. STA 4	2.0(50.8)	0.432 (10.97)	15 (66.7)	1.5 (6.67)	69,000
PLATE V, LONG., STA 4	2.0(50.8)	0.422 (10.72)	15 (66.7)	1.5 (6.67)	91,900

59
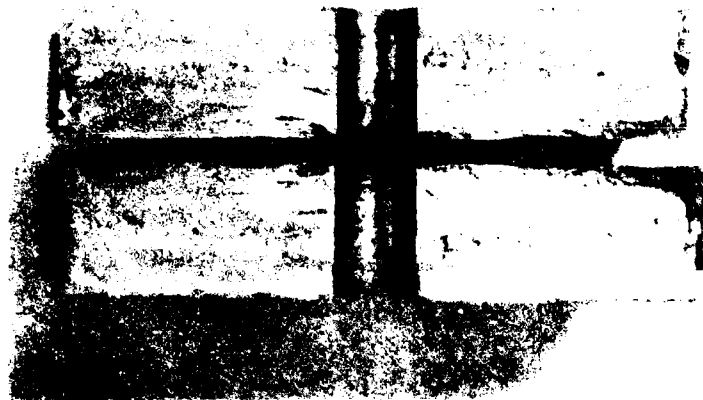
10 mm

FIGURE 25. MATING FRACTURE SURFACES OF Ti-10,2,3 STA 4
TENSION PANEL TESTED TO FAILURE IN FATIGUE.
MAGNIFICATION: 1X.
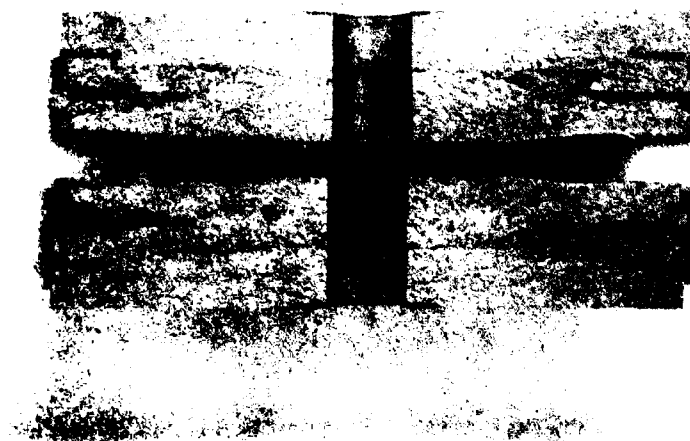
10 mm

FIGURE 26. MATING FRACTURE SURFACES OF PLATE V (Ti-10,2,3,/Ti-15,3,3,3)
STA 4 TENSION PANEL TESTED TO FAILURE IN FATIGUE.
MAGNIFICATION: 1X.

60

structural item fabricated from a roll-bonded laminate. In all cases, the improvement in properties results from the retention through lamination of thin plate properties in thick section. This property of laminates effectively allows their fracture behavior to operate mechanically as if they were always of thin section size, i.e., as if they were in plane stress rather than plane strain. This, in turn, allows the laminates to absorb more energy through plastic deformation during fracture. In addition, as shown through the bonding and testing of the 300M/E52100 laminate, laminates may be fabricated to possess other desirable properties, such as wear resistance, without seriously compromising their fracture toughness at least in the crack divider orientation.

4.0 CONCLUSIONS

The present investigation has demonstrated that roll-bonded metal-metal laminates offer fracture toughness and fatigue strength advantages over conventional monolithic or homogeneous alloys in thick section structures. This improvement in toughness results from the retention of individual layer or thin section fracture properties in the laminates through the operation of controlled delamination during fracture. As a result, laminates possess the elastic properties and strength of a monolithic material with much improved fracture toughness. Since it is fracture toughness, not ultimate strength, which determines the usable strength of any structural item, laminates may be utilized at higher working loads, or concomitantly, laminates possess greater damage tolerance, the ability to withstand a service induced flaw at equivalent working loads.

The techniques for roll bonding steel and titanium alloy laminates developed in the present program have the potential for commercial exploitation and can be especially cost effective if further optimization of the technology is effected. Roll bonding has been demonstrated to be a viable technique for the fabrication of multilayer laminate plate using dissimilar alloy layers within a given alloy system, e.g., alloy steels laminated to other alloy or carbon steels. Furthermore, the roll-bonding procedures developed are applicable to even very reactive materials, such as titanium alloys.

The fabricability of metal-metal laminates coupled with the improved fracture toughness obtainable through lamination make these laminates effective candidates for high strength structural items requiring a high degree of damage tolerance or resistance to fracture.

In summary, the following conclusions are justified:

- Roll bonding at elevated temperatures has been demonstrated to be a viable technique for the fabrication of multilayer laminate plate.

- Both steel alloys and titanium alloys have been successfully roll bonded. The primary steel alloy investigated has been 300M bonded to 1020, 1075, and E52100 steels. Three titanium alloys (Ti-6Al-4V, Ti-3Al-8V-6Cr-4Zr-4Mo, and Ti-10V-2Fe-3Al) have been roll bonded to various titanium alloy interleaves.

- For properly selected layer and interleaf combinations and mechanical and thermal processing conditions, both steel and titanium laminates may be fabricated such that the critical fracture toughness of the laminate is at least equal to the fracture toughness of the individual layers. This results from the retention of thin layer properties in thick section.

- The toughness improvement in the laminates resulted from a controlled delamination during fracture which separated the layers and allowed them to behave independently.

- Although the principal fracture toughness improvement was due to the retention of individual layer properties and the concomitant plane stress or nearly plane stress fracture, the properties of the interleaf alloy between the primary alloy layers were of key importance in the control of the tensile and fracture properties of the laminate. Specifically, the mating of a strong, brittle primary layer alloy with a weaker, ductile interleaf produced the largest relative benefit in improved toughness.

- In addition to fracture toughness the fatigue strength of simulated structural items fabricated from laminates was demonstrated to be superior to identical items fabricated from the same alloy in monolithic form.

- Since the layer and interleaf alloys are different, they may be chosen such that property control of a laminate may be effected through heat treatment alone. This allows property tailoring and optimization in an individual metal-metal laminate.

5.0 RECOMMENDATIONS

In addition to the properties evaluated in the present study, roll bonded steel and titanium laminates may also have fatigue, corrosion-fatigue, and stress corrosion properties which are superior to the corresponding monolithic materials. These properties need to be evaluated and compared in order to effectively evaluate the potential usefulness of laminates. Furthermore, more design specific data, such as fatigue strength, crack propagation rate, and general property variation need to be evaluated for the laminates. Finally the effects of forming processes, such as forging, extrusion, and post-bond rolling, on the properties of laminates need to be examined.

The fatigue and corrosion-fatigue crack propagation properties of roll-bonded laminates should be investigated in more detail for both the crack arrest and crack divider orientations. In both cases, there is potential for improved crack propagation resistance through the proper design and heat treatment of the laminates.

For equivalent reasons to those for the recommended corrosion-fatigue investigation, the stress corrosion cracking properties of laminates should be examined. In particular, the crack arrest orientation in laminates may offer superior stress corrosion properties if the interleaf alloy and heat treatment are chosen such that the interleaf acts as a chemical or mechanical barrier to stress corrosion crack advance.

The effects of post-bonding forming processes, in particular forging, on the mechanical properties of roll-bonded laminates should be investigated. Since such processes will be required in order to form many usable items from laminates, their effects should be known. Furthermore, some property enhancement may be possible through changes in material orientation and flow as a result of post-bonding forming processes.

The individual layer and interleaf properties as well as the processing conditions which control the properties of a roll-bonded laminate as a whole need to be analytically modeled. Such modeling could be of use in the efficient tailoring and optimization of metal-metal laminates for specific purposes. In addition, this modeling could serve to clarify the primary variables responsible for mechanical property improvement in metal-metal laminates and lead to further property enhancement through lamination.

64

Since roll bonding has been demonstrated to be a viable technique for joining titanium alloys, it should be exploited through the optimization of interleaf alloy selection and laminate heat treatment. There appears to be further benefit obtainable in the Ti-10,2,3/Ti-15,3,3,3 system through heat treatment optimization, for instance. In addition, the selection of an interleaf material with extensive inherent ductility, such as a non-heat treatable alpha alloy, or one in which ductility is transformation induced, such as the Transage* alloys, may provide a very large incremental increase in toughness without complex heat treatment.

* Transage is a trademark of the Lockheed Missiles and Space Company.

6.0 REFERENCES

1. H. L. Leichter, "Impact Fracture Toughness and Other Properties of Brazed Metallic Laminates," J. Spacecraft 7 (3), 1113 (1966).

2. J. D. Embury, N. J. Petch, A. E. Wraith, and E. S. Wright, "The Fracture of Mild Steel Laminates," Trans. AIME 239, 114 (1967).

3. J. G. Kaufman, "Fracture Toughness of 7075-T6 and -T651 Sheet, Plate, and Multilayered Adhesive-Bonded Panels," J. Basic Engr., Trans. ASME, 89, Series D (3), 503 (1967).

4. R. F. McCartney, R. C. Richard, and P. S. Trozzo, "Fracture Behavior of Ultrahigh-Strength-Steel Laminar Composites," Trans. ASM 60, 384 (1967).

5. E. A. Almond, J. D. Embury, and E. S. Wright, "Fracture in Laminated Materials," Interfaces in Composites, ASTM STP 452 (American Society for Testing and Materials, Phila.), 107 (1969).

6. S. D. Antolovich, K. Kasi, and G. R. Chanani, "Fracture Toughness of Duplex Structures: Part II - Laminates in the Divider Orientation," Fracture Toughness, Proceedings of the 1971 National Symposium on Fracture Mechanics, Part II, ASTM STP 514 (American Society for Testing and Materials, Phila.), 135 (1972).

7. D. Cox and A. S. Tetelman, Improved Fracture Toughness of Ti-6Al-4V Through Controlled Diffusion Bonding, Air Force Materials Laboratory Technical Rept. AFML-TR-71-264, (1972).

8 D. O. Cox and A. S. Tetelman, Fracture Toughness and Fatigue Properties of Titanium Laminate Composites Produced by Controlled Diffusion Bonding, Air Force Materials Laboratory Technical Rept. AFML-TR-73-288, (1973).

9. S. D. Antolovich, G. R. Chanani, A. Saxena, and I. C. Wang, "Fracture Mechanism Transitions in Laminate Composites," J. Phys. D: Appl. Phys. 6, 560 (1973).

10. A. A. Anctil, R. Chait, C. H. Curll, and E. B. Kula, Structural Properties of Dual Hardness Steel Armor, Army Materials and Mechanics Research Center Technical Rept. AMMRC TR 73-6, (1973)

11. E. B. Kula, A. A. Anctil, and H. H. Johnson, Fatigue and Crack Growth in Dual-Hardenss Steel Armor, Army Materials and Mechanics Research Center Technical Rept. AMMRC TR 74-6, (1974).

12. N. G. Ohlson, "Fracture Toughness of Laminated Steels," Eng. Fract. Mech. 6, (3), 459 (1974).

13. T. M. Devine, S. F. Floreen, and H. W. Hayden, "Fracture Mechanisms in Maraging Steel-Iron Laminates," Eng. Fract. Mech. 6 (2), 315 (1974).

14. S. Floreen, N. Kenyon, and H. W. Hayden, "The fabricability and Toughness of Laminar Composites of Maraging Steel," Trans. ASME, J. Engr. Mater. Tech. Vol. 96, Series H (3), 176 (1974).

15. J. F. Troop and J. F. Miller, <u>Fatigue Behavior of Metal Laminates,</u> Watervliet Arsenal Technical Rept. WVT-TR-75035, (1975).

16. P. T. Lum, R. Chait, and C. F. Hickey, Jr., "The Toughness of High Hardness Laminar Composite Steel as Influenced by Specimen and Crack Orientation," <u>Met. Trans. 6A</u>, 1093 (1975).

17. J. A. Alic, "Stable Crack Growth in Adhesively Bonded Aluminum Alloy Laminates," <u>Internl. J. Fracture 11</u> (4), 701 (1975).

18. R. R. Wells, <u>Low-Temperature Large-Area Brazing of Titanium Structures,</u> Air Force Materials Laboratory Technical Report AFML-TR-75-50, (1975).

19. S. J. Acquaviva and R. Chait, "The Effect of a Rising Tensile Load on Crack Extension in a Laminar Composite Steel, "<u>Met. Trans. 7A,</u> 1595 (1976).

20. J. A. Alic and A. Danesh, "Fracture of Laminates Combining 2024-T3 and 7075-T6 Aluminum Alloys," <u>Eng. Fract. Mech. 10</u> (2), 177 (1978).

21. R. D. Goolsby, "Fracture and Fatigue of Diffusion, Explosive, and Roll Bonded Al/Al and Ti/Ti Laminates," ATC Report No. B-94400/7CR-23, Prepared for Naval Air Systems Command on Contract No. N00019-76-C-0288, May 1977.

22. R. M. Johnson, "Fracture and Fatigue of Diffusion, Adhesive, and Roll Bonded Aluminum, Titanium, and Ultrahigh Carbon Steel Laminates," ATC Report No. B-92100/8CR-80, prepared for Naval Air Systems Command on Contract No. N00019-77-C-0287, May, 1978.

23. W. A. Reinsch and H. W. Rosenberg, "Three Recent Developments in Titanium Alloys," <u>Metal Progress, 117</u>(4), 64-69 (Mar 1980).

24. R. R. Boyer, "Design Properties of a High-Strength Titanium Alloy, Ti-10V-2Fe-3Al," <u>J. of Metals, 32</u> (3) 61-65 (March 1980).

25. "Military Specification: Steel Bars, Reforging Stock, and Mechanical Tubing Low Alloy, Premium Quality," MIL-S-8844C, 25 May 1971.

26. <u>Alloy Digest,</u> Engineering Alloys Digest, Inc. Upper Montclair, NJ.

27. "Military Specification: Titanium and Titanium Alloy, Sheet, Strip and Plate," MIL-T-9046H, 14 March 1974.

28 "Standard Methods of Tension Testing of Metallic Materials," ASTM E8-69, American Society for Testing and Materials, Philadelphia, PA, 1975.

29. "Standard Method of Test for Plane-Strain Fracture Toughness of Metallic Materials," ASTM E399-74, American Society for Testing and Materials, Philadelphia, PA, 1975.

30. H. Sunada, J. Wadsworth, J. Lin, and O. D. Sherby, "Mechanical Properties and Microstructure of Heat-Treated Ultrahigh Carbon Steels,"<u>Mat. Sci. and Eng., 38</u>, 35-40 (1979).

31. G. E. Dieter, _Mechanical Metallurgy_, McGraw-Hill, 1961, p. 246.

32. R. O. Ritchie, B. Francis, and W. L. Server, "Evaluation of Toughness in AISI Alloy Steel Austenitized at Low and High Temperatures," _Met. Trans._, _7A_, 831-838 (1976).

33. R. A. Wood, "Beta Titanium Alloys", MCIC 72-11, Metals and Ceramics Information Center, Columbus, OH, p. 167.

Department of the Navy
Naval Air Systems Command
Washington, D.C. 20361
Attn: Mr. W. T. Highberger
      AIR-5163C3 (10 copies)
      Mr. T. F. Kearns
      AIR-320
      Mr. R. A. Retta - AIR-5162C

Department of the Navy
Sea Systems Command
Washington, D. C. 20361
Attn: Code 03423

Chief of Naval Research
Department of the Navy
Washington, D.C. 20361
Attn: ONR 423, 471, (2 copies)

Commander
U.S. Naval Research Laboratory
Washington, D. C. 20390
Attn: Dr. Ray Hettche
      Dr. B. B. Rath

Commanding Officer
Naval Air Development Center,
      Johnsville
Aero Materials Laboratory
Warminster, Pennsylvania 18974
Attn: Mr. F. S. Williams

Naval Material Industrial Resources
      Office
Philadelphia, PA 19112

Air Force Materials Laboratory
Wright-Patterson Air Force Base
Dayton, Ohio 45433
Attn: Code: LTM (1 copy each)
Mr. Henry Johnson, Mr. Larry Clark
Mr. Ken Kojola, Mr. Lee Kennard,
Mr. A. M. Adair, LLM, Dr. Harry Lipsett

Army Research Office
Box CM, Duke Station
Durham, North Carolina 27706
Attn: Metallurgy and Ceramics Divison

Dr. F. H. Froes
Code: LLS
Air Force Materials Laboratory
Wright-Patterson AFB, OH 45433

Douglas Aircraft Company
3855 Lakewood Boulevard
Long Beach, CA 90846

National Academy of Sciences
National Materials Advisory Board
2101 Constitution Avenue
Washington, D.C. 20418
Attn: Dr. J. C. Lane

National Aeronautic and Space
      Administration
600 Independence Avenue
Washington, D.C. 20546

U.S. Army Materials & Mechanics
      Research Center
Watertown Arsenal
Watertown, Massachusetts 02172
Attn: Dr. E. S. Wright
      Dr. Eric Kula

Grumman Aerospace Corp.
Adv. Mat. & Processes
Bethpage, NY 11714
ATTN: Mr. Robert Witt

Battelle Memorial Institute
Defense Metals Information Center
505 King Avenue
Columbus, Ohio 43201
Attn: Mr. Thomas Byrer

Avco Space Systems Division
Lowell Industrial Park
Lowell, Massachusetts 01851

Brush Wellman, Inc.
17876 St. Clair Avenue
Cleveland, Ohio 44110

NASA/Langley
Attn: Mr. Tom Bales
Manufacturing Technology Section
Hampton, VA 23365

The Boeing Company
Aerospace Division
P. O. Box 3707, M/S 73-43
Seattle, Washington 98124
Attn: Mr. Rod Boyer

McDonnell Douglas Research Labs.
Attn: Dr. D. P. Ames
       Dr. Charles Witsett
St. Louis, Missouri 63166

Defense Doucmentation Center
Cameron Stations Bldg. 5
Alexandria, Virginia 22314
Attn: TCA (14 copies)
Via: Naval Air Systems Command
       Code AIR-954
       Washington, D.C. 20361

The Franklin Institute Research
       Laboratories
Twentieth & Parkway
Philadelphia, Pennsylvania 19103
Attn: Technical Director

Dr. John A. Schey
Department of Mechanical Engr.
University of Waterloo
Waterloo, Ontario
Canada N2L 3G1

Convair Division
General Dynamics
San Diego, California 92112
Attn: Mr. A. Hurlich

Dr. Charles Gilmore
School of Engineering and
       Applied Science
George Washington University
Washington, D.C. 20006

ITT Research Institute
10 West 35th Street
Chicago, Illinois 60616
Attn: Dr. N. Parikh

Kawecki Berylco Industries
P. O. Box 1462
Reading, Pennsylvania 19603
Attn: Dr. J. P. Denny

Ladish Company
Packard Avenue
Cudaby, Wisconsin 53110
Attn: Mr. Robert
       Mr. Daykin

Linde Company
Division of Union Carbide
P. O. Box 44
Tonawanda, New York 14152

Lockheed Aircraft Corporation
Lockheed Missile Systems Division
P. O. Box 501 - Orgn. 80-72, Bldg. 18
Sunnyvale, California 91088
Attn: Dr. M. I. Jacobson
       Dr. Frank Crossley

Lycoming Division
Avco Corporation
550 South Main Street
Stratford, Connecticut 06497
Attn: Division Library

Midwest Research Institute
425 Volker Boulevard
Kansas City, Missouri 64110

Northrop Corporation
3901 West Broadway
Hawthorne, California 90250
Attn: Mr. Allen Freedman
       Mr. T. R. Croucher
       Dr. Govind Chanani

Solar Division
Internation Harvester Company
2200 Pacific Highway
San Diego, California 92112
Attn: Dr. A. G. Metcalfe

United Aircraft Research Laboratory
East Hartford, Connecticut 06108
Attn: Mr. Roy Fanti

Vought Corporation
P. O. Box 225907
Dallas, Texas 75222
Technical Library

Dr. Paul Lowenstein
Nuclear Metals, Inc.
2229 Main Street
Concord, Massachusetts 01742

General Electric
Missile & Space Division
Materials Science Section
P. O. Box 8555
Philadelphia, Pennsylvania 91901
Attn: Technical LIbrary

Reynolds Metals Company
Reynold Metals Building
Richmond, Virginia 23218
Attn: Technical Library

Artech Corporation
2816 Fallfax Drive
Falls Church, Virginia 22042
Attn: Mr. Henry Hahn

General Electric Research Laboratory
Schenectady, New York 12301
Attn: Dr. Don Wood
        Mr. David Lillie (1 each)

Dr. Gary Gesehwind
Plant 26 (Research Dept.)
Grumman Aerospace Corporation
Bethpage, NY 11714

Mr. Carl Micillo
Grumman Aerospace Company
Adv. Mat. & Proc. Division
Bethpage, NY 11714

Aluminum Company of America
1200 Ring Bldg.
Washington, D.C. 20036
Attn: Mr. G. B. Barthold

Pratt & Whitney Aircraft Corp.
400 Main Street
East Hartford, Connecticut 06108
ATTN: Mr. George Rogers

Dr. Alan Lawley
Department of Metallurgical
   Engineering
Drexel University
32nd & Chestnut Streets
Philadelphia, Pennsylvania 19104

Dr. Howard Bomberger
Reactive Metals, Inc.
Niles, Ohio 44446

Massachusetts Institute of Technology
Department of Metallurgy and Material
  Science
Cambridge, Massachusetts 02139
Attn: Dr. N. J. Grant

Defense Advanced Research Project
   Agency
1400 Wilson Boulevard
Arlington, Virginia 22209
Attn: Dr. E. C. Van Reuth

Dr. Neil Paton
Rockwell Internation Corp.
Science Center
P. O. Box 1085
1049 Camino Dos Rios
Thousand Oaks, CA 91360

Pratt & Whitney Aircraft
Division of United Aircraft Corp.
Florida Research & Development Center
P. O. Box 2691
West Palm Beach, FL 33402
Attn: Mr. Joe Moore
        Mr. Marv Allen (1 each)

McDonnell Aircraft Co.
St. Louis, Missouri 63166
Attn: Mr. H. C. Turner

Dr. J. C. Williams
Department of Metallurgy and
  Material Science
Carnegie-Mellon University
Pittsburgh, Pennsylvania 15213

Lockheed Missiles & Space Company, Inc.
Palo Alto Research Laboratory
3521 Hanover Street
Palo Alto, California 94304
Attn: Dr. Thomas E. Tietz
      52-31/204

Titanium Metals Corporation of America
Henderson, Nevada 89015
Attn: Mr. James Hall

Grumman Aerospace Corporation
Bethpage, L.E., New York 11714
Attn: Mr. R. Heitzmann (2 copies)

Mr. George Hsu
Manager of Industry Standards
Reynolds Metals Corp.
6601 W. Broad Street
Richmond, Virginia 23261

Dr. John K. Tien
Henry Krumb School of Mines
Columbia University
New York, New York 10027

Boeing Vertol Company
Boeing Center
P.O. Box 16858
Philadelphia, Pennsylvania 19142

Mr. Gary Keller
D/115-050, SB04
Rockwell International
Los Angeles International Airport
Los Angeles, California 90009

Lockheed Aircraft
Attn: Mr. Rod Siemenz
Dept. 74-50, Bldg. 85
Burbank, CA 91520

Douglas Aircraft Company
3855 Lakewood Boulevard
Long Beach, CA 90846

Mr. A. E. Hohman, Jr.
Vought Corporation
P.O. Box 225907
Dallas, Texas 75266

Mr. R. G. Berryman
Air Research Co.
Mat'ls Application Group
93-3G1-503-4V
402 S. 36th St.
Phoenix, Arizona 85010

Titanium Metals Corp. of America
Attn: Mr. Larry Mayer
400 Rouser Road
P.O. Box 2824
Pittsburgh, PA 15230

Westinghouse Electric Corporation
Central Research Laboratories
Attn: Dr. Alan T. Male
Manager, Material Processing Research
Beulah Road, Churchill Borough
Pittsburgh, PA 15235

Wyman Gordon Co.
Attn: Mr. Charles Gure
Worcester Street
North Grafton, MA 05163

Crucible Materials Research Center
P.O. Box 88
Parkway West and Route 60
Pittsburgh, PA 15230
Attn: Mr. E. J. Dulis

Dr. D. H. Petersen
Vought Corporation
Advanced Technology Center
P.O. Box 226144
Dallas, Texas 75266

Army Aviation Systems Command
Attn: Mr. R. V. Vollmer
      AMSAV-ERE
P.O. Box 209
St. Louis, MO 63166

DATE
ILMED
—8